Increased abundance of proteins involved in resistance to oxidative and nitrosative stress at the last stages of growth and development of *Leishmania amazonensis* promastigotes revealed by proteome analysis.

Proteome profiling of *Leishmania amazonensis* promastigotes.

Pedro J. Alcolea[1*] (pjalcolea@cib.csic.es)

Ana Alonso[1] (amalonso@cib.csic.es)

Francisco García-Tabares[1] (fragata@cib.csic.es)

María C. Mena[2] (mcmena@cnb.csic.es)

Sergio Ciordia[2] (sciordia@cnb.csic.es)

Vicente Larraga[1] (vlarraga@cib.csic.es)

[1]Departamento de Microbiología Molecular y Biología de las Infecciones y Servicio de Proteómica y Genómica, Centro de Investigaciones Biológicas (Consejo Superior de Investigaciones Científicas), Calle Ramiro de Maeztu 9, 28040 Madrid, Spain.

[2]Unidad de Proteómica, Centro Nacional de Biotecnología (Consejo Superior de Investigaciones Científicas), Calle Darwin 3, 28049 Madrid, Spain.

*Corresponding author. Telephone: +34 918373112. Fax: +34 915360432. e-mail: pjalcolea@cib.csic.es

Keywords: cutaneous leishmaniasis; *Leishmania amazonensis*; promastigotes; differential gene expression; two-dimension electrophoresis; MALDI-TOF/TOF; arginase; iron superoxide dismutase; HSP70; LACK; rPKA; stress-inducible protein 1; tryparedoxin peroxidase.

Abstract.

Leishmania amazonensis is one of the major etiological agents of the neglected, stigmatizing disease termed american cutaneous leishmaniasis (ACL). ACL is a zoonosis and rodents are the main reservoirs. Most cases of ACL are reported in Brazil, Bolivia, Colombia and Peru. The biological cycle of the parasite is digenetic because sand fly vectors transmit the motile promastigote stage of the parasite to the mammalian host dermis during blood meal intakes. The amastigote stage survives within phagocytes of the mammalian host. The purpose of this study is detection and identification of differentially abundant proteins by 2DE/MALDI-TOF/TOF at different time points throughout growth and simultaenous differentiation of *L. amazonensis* promastigotes from the procyclic to the metacyclic stage. The average number of proteins detected per gel is 202 and the non-redundant cumulative number is 339. Of those, 63 are differentially abundant throughout growth and simultaneous differentiation of *L. amazonensis* promastigotes. The main finding is that certain proteins involved in resistance to nitrosative and oxidative stress (arginase, a light variant of the tryparedoxin peroxidase, iron superoxide dismutase, regulatory subunit of the protein kinase A and a light HSP70 variant) are more abundant at the last stages of growth and differentiation of cultured *L. amazonensis* promastigotes. These data taken together with the decrease of the stress-inducible protein 1 levels are additional evidence supporting the previously described pre-adaptative hypothesis, which consists of preparation in advance towards the amastigote stage.

Introduction.

American cutaneous leishmaniasis (ACL) is caused by 15 species of the genus *Leishmania* (Kinetoplastida: Trypanosomatidae), which includes species from the *Leishmania* and the *Viannia* subgenera. The latter is also able to cause mucocutaneous (MCL) leishmaniasis. *L. (L.) amazonensis* is one of the major etiological agents of ACL and it is grouped into the "*L. mexicana* complex". The initial ACL lesions are crater-shaped and they become ulcerated in the center with the progression of the disease. The species *L. mexicana*, *L. pifanoi* and *L. amazonensis* are also able to cause an infrequent form of the disease termed anergic diffuse cutaneous leishmaniasis (ADCL) [1], which is characterized by diffuse nodular lesions and total or partial anergy. ACL and ADCL are not life threatening, as a difference with visceral leishmaniasis (VL) caused by other species, but they are responsible for considerable morbidity.

According to the WHO epidemiological records, about 1.5 millon cases of CL are registered worldwide anually. Most ACL cases are concentrated in Brazil, Bolivia, Colombia and Peru [2,3]. A recent increase in the cases of leishmaniasis has been observed globally, which may be explained by many interrelated factors as scarce control, poverty, poor hygiene, migrations, return to rural areas, penetration into the jungle, changes in ambient humidity, deforestation, etc. ACL is a zoonosis and the major reservoirs are rodents when the etiological agents belong to the *L. mexicana* complex [2].

The life cycle of the parasite involves an invertebrate host that injects the motile promastigote stage of the parasite to the mammalian host when feeding from venules of the dermis. The vector belongs to the genus *Lutzomyia* (Psychodidae: Phlebotominae) in the case of New World species of the parasite such *L. amazonensis*. Promastigotes are engulfed by host phagocytes and differentiate to amastigotes. When a sand fly feeds

from blood of an infected mammal, amastigotes are released from phagocytes, transform into undifferentiated (procyclic) promastigotes and begin a developmental process from the procyclic to the more infective metacyclic stage.

A remarkable number of trypanosomatid genome sequences were assembled and annotated [4,5,6], which allowed for studying differential gene expression in different species, thus contributing to the knowledge about the biology of the parasite [7]. This is essential for future discovery of new drug targets and vaccine candidates. In the case of *L. amazonensis*, two-dimension electrophoresis (2DE) maps of promastigotes were described [8,9] and the effect of culture passage in the proteome of stationary phase promastigotes was evaluated by the same approach and in relation to the associated decrease of infectivity [10]. Also, a transcriptome analysis focused in the search of genes associated to antimony resistance was performed in promastigotes in mid-logarithmic growth phase of axenic culture [11], which is related to treatment strategies. However, differential gene expression throughout growth and development of the promastigote stage of *L. amazonensis* from the procyclic to the metacyclic stage has not been still explored. This is the aim of this study, which was performed by 2DE and subsequent matrix-assisted laser desorption-ionization tandem time-of-flight mass spectrometry (MALDI-TOF/TOF). The possible implications of the differentially abundant proteins found across growth and development of *L. amazonensis* promastigotes to the metacyclic stage is discussed herein.

Materials and methods.

Parasites.

Promastigotes of the *L. amazonensis* strain MHOM/Br/79/María were kindly provided by Alfredo Toraño and Mercedes Domínguez [12] and cultured at 27 ºC, pH 7.2 in liquid media composed of RPMI 1640 supplemented with L-glutamine (Life

Technologies, Carlsbad, CA), 10% heat inactivated fetal bovine serum (Lonza, Basel, Switzerland) and 100 μg/ml streptomycin – 100 IU/ml penicillin (Life Technologies). The initial cell density was adjusted to 2 x 10^6 cells/ml in all cultures and growth was registered daily at the light microscope using a Neubauer chamber. Culture samples containing 10^8 promastigotes were taken at the early-logarithmic, mid-logarithmic, late-logarithmic and stationary phases.

Total protein extracts.

Promastigotes (10^8 per sample) were harvested at 2,000 g for 10 min and washed once in PBS. Then, the sediment was carefully resuspended in 150 μl lysis buffer (8.4 M urea, 2.4 M thiourea, 5% CHAPS, 50 mM DTT, 1% Triton X-100, 50 μg/ml DNase and Mini EDTA-free Protease Inhibitor Cocktail according to the manufacturer's instructions –Roche, Mannheim, Germany) and immediately mixed by mild rotation at 4 ºC for 30 min. Then, the protein extracts were centrifuged at 8,000g for 10 min. The supernatant was recovered, precipitated with methanol/chloroform [13], dried at room temperature for 5 min and resuspended in 2X rehydration buffer (7 M urea, 2 M thiourea, 4% CHAPS, 0.003% bromophenol blue). Quantification was performed with the RC DC protein assay kit (BioRad) following the manufacturer's instructions and the results were compared with SDS-PAGE results as described [14].

Two-dimensional electrophoresis (2DE).

Fifty μg of total protein per sample were diluted to a final volume of 140 μl in 2X isoelectrofocusing (IEF) buffer (18.2 M DTT and 0.5% *IPG buffer solution* pH 3-10, BioRad). Then, samples were subject to IEF on 7 cm IPG pH 3-10 non-linear gradient strips (BioRad) in a Protean IEF Cell system (BioRad) following the manufacturer's instructions. Each run comprised seven steps (50 V for 12h, 250 V for 1h, 500 V for 1h, 1000 V for 1h, 2000 V for 1h, linear ramp to 8000 V for 1h and 8000 V up to 3500

V·h), reaching more than 12,000 V·h in every one. Then, the strips were run by 12% SDS-PAGE in a pre-cooled MiniProtean 3 Dodeca Cell system (BioRad) at 0.5 W/gel for 30 min and then at 1.5 W. The run was stopped 5 min after the die-front reached the bottom edge. The gels were stained with SYPRO Ruby (BioRad) and the gel images were acquired with EXQuest Spot Cutter (BioRad) according to the manufacturer's instructions.

The gel images were processed and analyzed with PDQuest 2D Advanced 8.0.1 software (BioRad) according to the manufacturer's instructions. First, the images were cropped and spots were detected automatically with the Spot Detection Parameter Wizard at a sensitivity value of 3.5. Then, all detected spots were manually checked by observation of 3D density graphs, single spot quantitation histograms and 2DE gel images. Normalization was performed by the Total Quantity in Valid Spots algorithm. Normality was checked by the Kolmogorov-Smirnov test and statistical inference of differential protein abundance was performed by the Student's t-test at the 0.05 significance level. Reproducibility was assured by preparing three independent biological replicate samples. However, all 2DE runs were performed simultaneously, which is essential for technical reproducibility across gels. For this purpose, all samples were stored at -80 ºC until use.

Protein identification by MALDI-TOF/TOF.

After excision of the selected spots with EXQuest Spot Cutter (BioRad), they were digested with trypsin and prepared for MALDI-TOF/TOF mass-spectrometry as described [14]. The digests were deposited in OptiTOF™ Plates (Life Technologies). Each well contained a 0.8 µl drop of peptides mixed with 0.8 µl of 3 µg/µl α-cyano-4-hydroxycinnamic acid (Sigma). The mixtures were allowed to dry at room temperature and run in an ABI 4800 MALDI-TOF/TOF mass spectrometer (Life Technologies) in

positive reflector mode at 25 kV for MS and 1 kV for MS/MS. The data obtained were analyzed with ABI 4000 Series Explorer software 3.6 (Life Technologies). Peptide mass fingerprinting (PMF) and MS/MS spectra of fragment ions were smoothed and corrected to the zero baseline using routines embedded in ABI 4000 Series Explorer Software v3.6. Each PMF spectrum was internally calibrated with the mass signals of trypsin autolysis ions to reach a typical mass measurement accuracy < 25 ppm. Known trypsin and keratin mass signals, as well as potential sodium and potassium adducts (+21 Da and + 39 Da) were removed from the peak list. Protein identifications were performed with MASCOT 2.1 using Global Protein Server Explorer 4.9 (Life Technologies). The following search parameters were introduced: enzyme, trypsin; allowed missed cleavages, 1; carbamidomethyl cystein as fixed modification by treatment with iodoacetamide; variable modifications, oxidation of methionine; mass tolerance was set to ± 50 ppm for precursors and to ± 0.3 Da for MS/MS fragment ions. The confidence interval for protein identification was set to ≥ 95% ($p < 0.05$) and only peptides with an individual ion score above the identity threshold (52) were considered correctly identified. The reference template for MASCOT identifications was the genome sequence of *L. mexicana* (http://tritrypdb.org/common/downloads/release-9.0/LmexicanaMHOMGT2001U1103/fasta/data/) because the genome of *L. amazonensis* has not been sequenced yet and this species is included in the "*L. mexicana* complex". All data were also run against against individual *L. amazonensis* sequences within the NCBInr database. The identifications are available in the PRIDE repository of the ProteomeXchange Consortium [15] with the accesion number PXD002939.

Results and discussion.

2DE-MS/MS analysis of *L. amazonensis* promastigotes.

Total protein was extracted from *L. amazonensis* axenic cultures of promastigotes at early-logarithmic (day 2), mid-logarithmic (day 3), late-logarithmic (day 5) and stationary (day 7) phase (Fig 1). Average protein concentrations (mg/ml) were: 4.4 ± 0.2 (day 2 promastigotes); 4.5 ± 0.4 (day 3); 4.4 ± 0.1 (day 5); 4.5 ± 0.2 (day 7). (Fig 2). The spots were automatically detected with the Spot Detection Parameter Wizard. Sensitivity was adjusted to 3.5 in order to filter out the non-identifiable faintest spots according to experimental setup with the mass spectrometer. An average of 202 spots were detected per gel and the cumulative non-reduntant number is 339 (S1 Table). The cut-off ratio values were 1.7 for up-regulation and 0.6 for down-regulation (1.7 and -1.7 fold changes), respectively (S1 Fig, S1 Table). Statistical significance was inferred with the Student's t test ($p < 0.05$) because the outcome of the Kolmogorov-Smirnov test was $p = 0.318$, 0.280 and 0.273 for the comparisons day3:day2, day5:day2 and day7:day2, respectively. Ratios are relative to early-logarithmic phase promastigotes (day 2). Sixty three differentially expressed proteins out of 339 could be identified by MALDI-TOF/TOF (Fig 2, Table 1, S1 Table) against the TriTrypDB *L. mexicana* genome annotations. All selected proteins were identified and the MASCOT score values were significant, except for one spot that could not be identified with the *L. mexicana* reference genome sequence but the NCBInr database instead (Table 2, spot Lam1601, soluble promastigote surface antigen fragment PSA-31S, part of the PSA-38S). In fact, this *L. amazonensis* gene had been previously characterized [16]. Random identification of constitutively expressed proteins was also performed (Table 2), which occasionally allowed retrieving additional information about relative expression in different pathways (see below). In certain cases, different spots contain the same protein, which may be due to protein processing, post-translational modifications or protein aggregation. In the next sections, this has been cited as "protein variant". In principle,

the nature of the variations is unknown but the 2DE-resolved variants could be separately analyzed and identified. The comparison of experimental and/or predicted molecular weight and isoelectric point provides insight (Table 3). For example, three variants of the protein LmxM.15.1160 were found. Two of them present a similar MW but differ in the estimated pI value in 0.5 pH units, whereas the MW of the third one is about 40% lower and the pI 8.5, which strongly suggests that a considerable portion of the protein sequence has been removed during processing. The most striking changes in experimental MW and pI (Table 3) are discussed below according to changes in relative abundance of variants of the same protein.

The differential gene expression results at the protein abundance level in the promastigote differentiation process studied herein are compared below with expression profiles reported in other species. Experimental variation between studies has been considered. In other cases, the information is complemented with reported data about the differentiation process of promastigotes to amastigotes.

Differential protein abundance in *L. amazonensis* promastigotes.

Regulation of gene expression.

Three variants of the translation elongation factor 2 (EF2) are up-regulated in mid-logarithmic with respect to early-logarithmic phase promastigotes, as well as two different DEAD/DEAH RNA helicases and the alanine-tRNA synthetase (Table 1). One of the EF2 is considerably lighter and slightly more basic (60.3 KDa, pI6.9) than the others (Table 3), which suggest that it is partially proteolyzed during processing. The two other variants may have been post-translationally modified, according to the difference with the theoretical MW value (Tables 1 and 3). A heavier variant of the EF2 is constitutively expressed (Table 2 and 3). This constitutive variant may present additional post-translational modifications, probably glycosylation regarding to the

increase in MW (Table 3). The increase in abundance of the EF2 variants (Tables 1 and 2) suggests changes in translational regulation at an intermediate point of growth and differentiation. The EF2 was described to be an immunostimulatory protein in *L. donovani* [17].

Another protein involved in gene expression regulation is the endoribonuclease L-PSP (pb5), which was found to be down-regulated in amastigotes of species causative of cutaneous (*L. mexicana*, *L. major*) and visceral (*L. donovani*, *L. infantum*) leishmaniasis [18,19,20,21,22]. However, information about differential abundance of this protein throughout promastigote growth and differentiation process is not available so far. In the case of *L. amazonensis*, this endoribonuclease is over-expressed in stationary phase promastigotes, therefore at the end of the differentiation process (Table 1).

These proteins are involved in translation and in post-transcriptional regulation of gene expression, a compendium of processes that has not been deeply characterized in these parasites and plays a key role in their biology because they lack most transcriptional regulation mechanisms (reviewed in [23]).

Protein folding.

The heat shock proteins HSP70 and HSP83-1 were described to be abundant and constitutive throughout the main stages of the life cycle of *Leishmania* spp. [24,25]. HSP70 proteins of *L. infantum* and *L. donovani* are immunostimulatory [17,26]. Differential expression in the promastigote stage of *L. infantum* was not detected at the transcript and protein levels [14,18]. In the case of *L. amazonensis*, distinct variants of both chaperones are constitutively or differentially expressed in promastigotes throughout growth and differentiation (Tables 1 and 2). Two HSP70 (LmxM.28.2770) variants of the same MW but different estimated pI (5.4 and 6.2) are less abundant at late-logarithmic phase (Tables 1 and 3). The HSP70-related protein 1 (HSP70-rel1),

encoded by a different gene (LmxM29.2490), is slightly heavier (Table 3) and its relative abundance is analogous, whereas a lighter variant of the LmxM.28.2770 HSP70 (44.5 KDa) of estimated pI around the theoretical value (5.2) is highly up-regulated (24-fold) in stationary phase promastigotes (Tables 1 and 3). Finally, a heavier variant (97.6 KDa) is constitutive (Tables 2 and 3). Therefore, alternation of HSP70 variants originated by protein processing or post-translational modifications is observed at the last stages of the growth and differentiation process of *L. amazonensis* promastigotes. Simultaneously, the chaperonin HSP60 is down-regulated (late-logarithmic phase), whereas the differentially regulated variants of the HSP83 are down-regulated at mid-logarithmic phase, an earlier point of growth and differentiation.

According to previous data, the stress-inducible protein 1 homolog (STI1) is constitutively expressed in the developmental process of stationary phase promastigotes to amastigotes in the case of *L. infantum* [27] but no information is available about growth and development of promastigotes from procyclics to metacyclics. In the case of *L. amazonensis*, the STI1 is down-regulated at late logarithmic phase (Table 1), simultaneously to some HSPs mentioned above.

Two variants of the η subunit of the T-complex protein 1 (TCP1η) are down-regulated in late logarithmic phase promastigotes, whereas the TCP1β subunit is constitutively expressed (Table 2). Therefore, the down-regulation of the TCP1η, the STI1 and the HSPs mentioned above is simultaneous and takes place at one of the final stages of growth and differentiation of *L. amazonensis* promastigotes in culture. The exact function of the TCP complex is not known in *Leishmania* spp., although it has been suggested that the TCP1γ subunit may participate in maintaining the structural dynamics of the cytoskeleton [28]. Changes in cell morphology accross promastigote differentiation and flagellar movement demand continuous re-organization of the

cytoskeleton. Differential expression of the TCP1η has not been reported in *L. infantum* promastigotes differentiating from procyclics to metacyclics in culture so far, although the encoding gene is up-regulated at the transcript level in metacyclic promastigotes isolated from the sand fly anterior midgut according to a recent study [29].

A cyclophilin variant is down-regulated in mid-logarithmic phase *L. amazonensis* promastigotes, whereas another variant is constitutively expressed. Cyclophilins are able to prevent aggregation of adenosine kinase domain-containing proteins [30,31] like nucleoside diphosphate kinases (NDK). Two NDKb variants encoded by the same gene but very different in MW (presumably due to processing) are up-regulated at the beginning of growth and differentiation of promastigotes (early-logarithmic phase) (Tables 1 and 3). Up-regulation of the NDKb at the transcript level in procyclic *L. infantum* promastigotes [32] agrees with the profile found in *L. amazonensis*. The NDKs are involved in nucleotide biosynthetic processes, which may occur preferentially at the initial stages of growth and differentiation of promastigotes as suggested by the results. The 14-3-3 protein 1 relative abundance profile is the same as for the NDKb in *L. amazonensis* promastigotes. The exact functions of 14-3-3 proteins are unknown, although they have been related to many cellular processes. An intrinsic NDK activity has been associated to these proteins in general [33] and antiapoptotic properties of the *L. donovani* orthologs have been reported [34]. In fact, the 14-3-3 protein is able to prolong the lifespan of the infected host phagocyte. Given the multiple functions of this protein, the implications of its increased levels at the beginning of promastigote growth and differentiation is not known so far.

Proteolysis.

Two components of the ubiquitin-proteasome system are differentially abundant throughout growth and differentiation of *L. amazonensis* promastigotes: the ubiquitin-

conjugating enzyme E2 (UbqC-E2) is down-regulated in late-logarithmic phase, whereas the proteasome α-3 subunit is up-regulated in stationary phase promastigotes (Table 1). None of them have been detected in differential gene expression analysis during development of promastigotes of any *Leishmania* species in culture so far. However, it has been described that the the E2 steady-state transcript levels are higher in cultured promastigotes than in promastigotes obtained from the sand fly gut [29,35]. The 14-3-3 protein is associated to other components of the proteasome [36]. As mentioned above, the abundance of this protein decreases at the last stages of growth and development of *L. amazonensis* promastigotes (late-logarithmic phase promastigotes), which is simultaneous to the decrease of the UbqC-E2.

Other proteases of unknown function are differentially abundant throughout growth and development of *L. amazonensis* promastigotes. Two mitochondrial protein peptidase variants and a metal-dependent aminoexopeptidase of the M17 family are up-regulated in mid logarithmic phase, whereas the calpain LmxM.20.1280 is down-regulated in late-logarithmic phase promastigotes. Up-regulation at the transcript level of a different calpain gene of *L. infantum* (LinJ.20.1230) in metacyclic promastigotes was reported [32]. Two variants of a mitochondrial processing peptidase of the M16 family are up-regulated at day 3 (mid-logarithmic phase) and they present similar MW and pI analogous to the theoretical value (Table 3).

Signaling.

The protein kinase A (PKA) of *L. amazonensis* was described to be involved in autophagy [37,38], which is a critical process in promastigote differentiation. This is in agreement with 24-fold increase of the regulatory subunit (rPKA) in stationary phase promastigotes of this species (Table 1). The rPKA is also up-regulated at the transcript level at the same growth phase of *L. infantum* promastigotes [18]. Therefore, these data

point to an increase of abundance of the rPKA upon growth and differentiation of the promastigote stage, which may be critical for survival.

The receptor of the activated protein kinase C (RACK) of *Leishmania* spp. (LACK) is up-regulated in early-logarithmic phase promastigotes in *L. amazonensis* (Table 1). Constitutive expression throughout growth of *L. infantum* promastigotes has been reported [39]. The motile stage of *Crithidia fasciculata*, a monogenetic trypanosomatid that does not infect mammals in its life cycle, also increases the levels of the RACK orthologue CACK in early logarithmic phase [40] like *L. amazonensis*, according to 2DE-MALDI-TOF/TOF results obtained by the same procedure. The LACK antigen is able to protect partially against canine leishmaniasis when the encoding gene is administered in a mammalian expression plasmid vector either containing antibiotic resistance genes or alternative selection markers [41]. This protein is located in the particulate fraction of the cytoplasm near the plasma membrane and it is up-regulated in *L. infantum* amastigotes [39]. RACK proteins belong to the WD40 repeat family. In particular, LACK is able to bind sequences present in certain proteins involved in DNA replication and RNA synthesis and the β chain of the MHC II. RACKs are able to translocate PKCs to the required intracellular locations [24] in order to participate in certain signal transduction pathways that have been characterized in mammalian cells [25]. The current knowledge on signal transduction pathways is still reduced in trypanosomatids. However, progress has been made with particular proteins. For example, at least one of the rPKA functions could be determined (autophagy, involved in metacyclogenesis) and it is known that LACK is a good vaccine candidate [41]. The signaling proteins 14-3-3 and putative protein phosphatase in Table 1 are more abundant in early logarithmic phase. The 14-3-3 protein is also involved in protein

348 folding. As mentioned above, antiapoptotic function able to prolong the lifespan of the
349 infected macrophage has been also described [34].

350 **Catabolism and biosynthesis of surface molecules.**

351 Glycolysis is especially important for trypanosomatid parasites [42,43,44]. The triose
352 phosphate isomerase (TPI), the enolase and the bisphosphoglycerate-independent
353 phosphoglycerate mutase (PGM^{BPI}) are differentially regulated in *L. amazonensis*
354 promastigotes (Table 1), whereas the glyceraldehyde-3-phosphate dehydrogenase
355 (gGAPDH) is constitutively expressed (Table 2). Constitutive expression of the
356 gGAPDH was also described in the differentiation process of *L. infantum* promastigotes
357 to amastigotes [27]. The abundance of the TPI, a potential vaccine candidate [45],
358 decreases in mid-logarithmic phase promastigotes, whereas the PGM^{BPI} is up-regulated
359 at late-logarithmic phase. The PGM^{BPI} was reported to be down-regulated in *L. infantum*
360 and *L. donovani* amastigotes [18,21,22,46] at the transcript and protein levels,
361 respectively. Additionally, this protein is considered a promising drug target candidate
362 [47]. Differential expression of the TPI and the PGM^{BPI} has not been detected across
363 promastigote growth and differentiation of these visceral leishmaniasis-causative
364 species in other studies. The enolase is down-regulated at the final stages of growth and
365 differentiation of *L. amazonensis* (late-logarithmic phase) (Fig 3), which is analogous at
366 the transcript level (over-expressed in metacyclics) in the case of *L. infantum* [32]. This
367 protein is down-regulated in the amastigote stage of *L. mexicana*, *L. donovani* and *L.*
368 *infantum* [19,21,22,32]. The expression profile in *L. infantum* stationary phase
369 metacyclic promastigotes is comparable at the transcript level [32].

370 Three components of the pyruvate dehydrogenase complex (PDC), namely the E1β
371 subunit, dihydrolipoamide dehydrogenase (DHLDH) and dihydrolipoamide
372 acetyltransferase (DHLAT), are significantly up-regulated in early-logarithmic phase

promastigotes (Fig 3, Table 1). The aconitase is the only differentially abundant enzyme of the Krebs cycle found. This protein is over-expressed at the beginning of growth and differentiation of promastigotes (in early-logarithmic phase), like the PDC components mentioned above. On the opposite, the citrate synthase (CitS), isocitrate dehydrogenase (ICDH), succinyl-CoA synthetase α subunit (SCS) and GDP-forming succinyl-CoA ligase β chain (SCL) are constitutively expressed (Fig 3, Table 2).

The Rieske iron sulfur precursor (RISP) is a protein involved in the electron transport chain. RISP abundance decreases in late-logarithmic phase promastigotes, when growth and differentiation are at an advanced stage. In summary, the differentially abundant glycolytic enzymes TPI and enolase, the DHLDH and DHLAT components of the PDC and the electron transport chain protein RISP are down-regulated in the final stages of growth and differentiation of promastigotes. This suggests a higher demand of energy during the first stages of development. On the opposite, the acyl-CoA dehydrogenase, involved in β-oxidation of fatty acids, is up-regulated in stationary phase promastigotes, which suggests alternation between the sugar and lipid catabolism. The expression pattern of the cofactor-independent PGM^{BPI} is also different. However, protists and eubacteria also contain the cofactor-dependent PGM, including trypanosomatids [48,49]. The enoyl-CoA hydratase/isomerase (ECH) is down-regulated in mid-logarithmic phase promastigotes and participates in the metabolism of unsaturated fatty acids. Finally, the 5-methyltetrahydropteroyltriglutamate-homocysteine methyltransferase (MET6), an enzyme that participates methionine metabolism, is up-regulated at mid logarithmic phase (Fig 3, Table 1).

The GDP-mannose pyrophosphorylase (GDP-MP) is up-regulated in late-logarithmic phase promastigotes, which is in agreement with a previous observation in *L. infantum* promastigotes by the same approach [14]. The GDP-MP is essential for virulence of

promastigotes of *L. mexicana* [50], a species closely related to *L. amazonensis*. This enzyme is involved in biosynthesis of the lipophosphoglycan (LPG), the glycosylinositol phospholipids (GIPLs) and other glycoconjugates characteristic of the surface of these parasites. The up-regulation of the GDP-MP in late-logarithmic phase promastigotes suggests that higher amounts of these surface molecules are synthesized when the end of growth and differentiation of promastigotes approaches.

Up-regulation of proteins involved in resistance and survival at the last stages of growth and development of *L. amazonensis* promastigotes.

Trypanothione system.

A processed protein variant (12.9 KDa, pI8.5) of the tryparedoxin peroxidase (TryP) is constitutively expressed throughout the growth curve of *L. amazonensis* promastigotes, whereas two heavier variants of estimated experimental MW and pI close to the theoretical values (22.0 KDa, pI6.0) are differentially abundant (Fig 4, Tables 1 and 3). One of the TryP heavy variants is up-regulated at day 3, whereas the other one is down-regulated at the same time point. The TryP light variant is highly up-regulated (>30-fold) in stationary phase promastigotes (day 7). In the case of *L. infantum*, the TryP decreases in amastigotes compared to promastigotes [27] but there are no available data about relative abundance during growth and differentiation process of amastigotes to date.

The complex expression profile of different TryP variants in *L. amazonensis* promastigotes (Figure 4) has not been found in Old World leishmania species such as *L. major* or *L. infantum* so far and the enzyme was reported to be constitutively expressed in both species [18,51], whereas the non-pathogenic trypanosomatid *C. fasciculata* differentially regulates the TryP accross growth and differentiation of the motile choanomastigote stage [40]. In addition to cellular detoxification of reactive oxygen

423 species, the TryP has been involved in other processes such signaling proliferation and
424 differentiation [52]. The complex expression pattern of different variants found in *L.*
425 *amazonensis* promastigotes (Figure 4) suggests that the TryP is especially important
426 throughout the growth and differentiation process studied herein.
427 The iron superoxide dismutase (Fe-SOD) is over-expressed in *L. amazonensis* and in *C.*
428 *fasciculata*. This protein initiates elimination of the superoxide anion by conversion to
429 hydrogen peroxide. The Fe-SOD is up-regulated in *L. amazonensis* late logarithmic
430 phase promastiogtes (day 5). The TryP is able to reduce this substrate thanks to the
431 assistance of the tryparedoxin (TXN1), the trypanothione ($T[S]_2/T[SH]_2$) and the
432 NADPH-dependent enzyme trypanothione reductase (TryR). The TryR has not been
433 identified between the selected spots of this analysis and the TXN1 is among the
434 constitutively expressed ones (Table 2).
435 **Arginase.**
436 The arginase is a manganese-dependent enzyme that participates in the urea cycle by
437 hydrolyzing L-arginine into urea and ornithine. These products are able to induce the
438 alternative macrophage activation pathway [53]. The ARG of the host phagocytic cell
439 competes with the inducible nitric oxide synthase (iNOS) for the substrate L-arginine
440 [54]. For these reasons, parasite clearance is more effective when low levels of host
441 ARG are expressed. The ARG is also annotated in the genomes of the *Leishmania*
442 species, thus contributing to decrease the levels of NO synthesis by the iNOS of the host
443 cell through substrate competence. This enzyme is essential for infectivity, proliferation
444 and virulence of the parasite [55,56]. 2DE-MALDI-TOF/TOF analysis has revealed
445 high ARG levels (29-fold) in *L. amazonensis* stationary phase promastigotes. *L.*
446 *infantum* promastigotes over-express the ARG in amastigotes with respect to stationary
447 phase promastigotes [27]. A possible explanation for these findings combined is

448 preparation in advance for differentiation to the amastigote stage and survival within the
449 phagolysosome of the host cell. This statement is called pre-adaptation hypothesis and
450 has been previously supported [18,57,58,59].
451 Ornithine is also an essential precursor in polyamine biosynthesis [54, 55]. This
452 pathway is essential for the biosynthesis of trypanothione because this molecule consists
453 of two glutathione residues coupled through spermidine. Consequently, arginase up-
454 regulation might be indirectly related to the TryP differential expression profile
455 described (Fig 4).
456 **Synopsis of differentially abundant proteins involved in survival and resistance.**
457 The decreased abundance of a variant of the STI1 chaperone simultaneous to the
458 increase of the levels of the ARG, HSP70, TryP, Fe-SOD (stress-resistance genes) and
459 rPKA (indicative of differentiation), when growth and differentiation of *L. amazonensis*
460 promastigotes has been completed, is in agreement with the pre-adaptation hypothesis
461 towards survival within the host phagocyte. In addition, higher levels of the GDP-ManP
462 have been observed at an advanced growth phase, which probably leads to increased
463 amounts of glycoconjugates in differentiated promastigotes.

464 ## Conclusions.

465 2DE-MS/MS has revealed that promastigotes of the New World species *L.*
466 *amazonensis*, responsible for ACL, up-regulate proteins involved in survival and
467 resistance throughout growth and development in culture: the TryP and the Fe-SOD,
468 involved in defense against oxidative damage; the ARG, involved in nitrosative stress
469 resistance within the phagocytic host cell, whose up-regulation in stationary phase
470 promastigotes may be explained by the pre-adaptative hypothesis; the
471 immunostimulatory protein HSP 70, involved in protein folding; and the rPKA,
472 involved in signaling and autophagy, thus related with metacyclogenesis. The LACK

antigen is down-regulated throughout growth and simultaneous development of promastigotes in this species causative of ACL, whereas it was reported to be constitutively expressed in the VL agent *L. infantum*. The down-regulation of the STI1 and the up-regulation of proteins involved in resistance and survival (ARG, HSP70, Fe-SOD, TryP and rPKA) in fully grown and differentiated promastigotes suggest the pre-adaptative hypothesis, also proposed for other *Leishmania* species.

Acknowledgements.

We would like to express our gratitude to Alfredo Toraño and Mercedes Domíngez for their advice and support, as well as for lending us the *L. amazonensis* strain studied in this proteome analysis.

References.

1. Convit J, Lapenta P (1946) Sobre un caso de leishmaniasis diseminada. Rev Pat Clin 17: 153-158.
2. WHO (2010) Report of a Meeting of the WHO Expert Committee on the Control of Leishmaniases. . Geneva.
3. WHO (2015) Leishmaniases. Epidemiological Report of the Americas. Report Leishmaniases.
4. Ivens AC, Peacock CS, Worthey EA, Murphy L, Aggarwal G, et al. (2005) The genome of the kinetoplastid parasite, Leishmania major. Science 309: 436-442.
5. Peacock CS, Seeger K, Harris D, Murphy L, Ruiz JC, et al. (2007) Comparative genomic analysis of three Leishmania species that cause diverse human disease. Nat Genet 39: 839-847.
6. Aslett M, Aurrecoechea C, Berriman M, Brestelli J, Brunk BP, et al. (2010) TriTrypDB: a functional genomic resource for the Trypanosomatidae. Nucleic Acids Res 38: D457-462.
7. de Toledo JS, Vasconcelos EJR, Ferreira TR, Cruz AK (2010) Using Genomic Information to Understand Leishmania Biology. Open Parasitol J 4: 156-166.
8. Brobey RK, Mei FC, Cheng X, Soong L (2006) Comparative two-dimensional gel electrophoresis maps for promastigotes of Leishmania amazonensis and Leishmania major. Braz J Infect Dis 10: 1-6.
9. Brobey RK, Soong L (2007) Establishing a liquid-phase IEF in combination with 2-DE for the analysis of Leishmania proteins. Proteomics 7: 116-120.
10. Magalhaes RD, Duarte MC, Mattos EC, Martins VT, Lage PS, et al. (2014) Identification of differentially expressed proteins from Leishmania amazonensis associated with the loss of virulence of the parasites. PLoS Negl Trop Dis 8: e2764.
11. do Monte-Neto RL, Coelho AC, Raymond F, Legare D, Corbeil J, et al. (2011) Gene expression profiling and molecular characterization of antimony resistance in Leishmania amazonensis. PLoS Negl Trop Dis 5: e1167.

12. Dominguez M, Torano A (2001) Leishmania immune adherence reaction in vertebrates. Parasite Immunol 23: 259-265.
13. Wessel D, Flugge UI (1984) A method for the quantitative recovery of protein in dilute solution in the presence of detergents and lipids. Anal Biochem 138: 141-143.
14. Alcolea PJ, Alonso A, Larraga V (2011) Proteome profiling of Leishmania infantum promastigotes. J Eukaryot Microbiol 58: 352-358.
15. Vizcaino JA, Deutsch EW, Wang R, Csordas A, Reisinger F, et al. (2014) ProteomeXchange provides globally coordinated proteomics data submission and dissemination. Nat Biotechnol 32: 223-226.
16. Bras-Goncalves R, Petitdidier E, Pagniez J, Veyrier R, Cibrelus P, et al. (2014) Identification and characterization of new Leishmania promastigote surface antigens, LaPSA-38S and LiPSA-50S, as major immunodominant excreted/secreted components of L. amazonensis and L. infantum. Infect Genet Evol 24: 1-14.
17. Gupta SK, Sisodia BS, Sinha S, Hajela K, Naik S, et al. (2007) Proteomic approach for identification and characterization of novel immunostimulatory proteins from soluble antigens of Leishmania donovani promastigotes. Proteomics 7: 816-823.
18. Alcolea PJ, Alonso A, Gomez MJ, Moreno I, Dominguez M, et al. (2010) Transcriptomics throughout the life cycle of Leishmania infantum: high down-regulation rate in the amastigote stage. Int J Parasitol 40: 1497-1516.
19. Holzer TR, McMaster WR, Forney JD (2006) Expression profiling by whole-genome interspecies microarray hybridization reveals differential gene expression in procyclic promastigotes, lesion-derived amastigotes, and axenic amastigotes in Leishmania mexicana. Mol Biochem Parasitol 146: 198-218.
20. Leifso K, Cohen-Freue G, Dogra N, Murray A, McMaster WR (2007) Genomic and proteomic expression analysis of Leishmania promastigote and amastigote life stages: the Leishmania genome is constitutively expressed. Mol Biochem Parasitol 152: 35-46.
21. Rosenzweig D, Smith D, Myler PJ, Olafson RW, Zilberstein D (2008) Post-translational modification of cellular proteins during Leishmania donovani differentiation. Proteomics 8: 1843-1850.
22. Rosenzweig D, Smith D, Opperdoes F, Stern S, Olafson RW, et al. (2008) Retooling Leishmania metabolism: from sand fly gut to human macrophage. FASEB J 22: 590-602.
23. Clayton C, Shapira M (2007) Post-transcriptional regulation of gene expression in trypanosomes and leishmanias. Mol Biochem Parasitol 156: 93-101.
24. Zilberstein D, Shapira M (1994) The role of pH and temperature in the development of Leishmania parasites. Annu Rev Microbiol 48: 449-470.
25. Wiesgigl M, Clos J (2001) The heat shock protein 90 of Leishmania donovani. Med Microbiol Immunol 190: 27-31.
26. Carrillo E, Crusat M, Nieto J, Chicharro C, Thomas Mdel C, et al. (2008) Immunogenicity of HSP-70, KMP-11 and PFR-2 leishmanial antigens in the experimental model of canine visceral leishmaniasis. Vaccine 26: 1902-1911.
27. Lynn MA, Marr AK, McMaster WR (2013) Differential quantitative proteomic profiling of Leishmania infantum and Leishmania mexicana density gradient separated membranous fractions. J Proteomics 82: 179-192.
28. Bhaskar, Mitra K, Kuldeep J, Siddiqi MI, Goyal N (2015) The TCP1gamma subunit of Leishmania donovani forms a biologically active homo-oligomeric complex. FEBS J 282: 4607-4619.
29. Alcolea PJ, Alonso A, Dominguez M, Parro V, Jimenez M, et al. (2016) Influence of the Microenvironment in the Transcriptome of Leishmania infantum Promastigotes: Sand Fly versus Culture. PLoS Negl Trop Dis 10: e0004693.
30. Chakraborty A, Sen B, Datta R, Datta AK (2004) Isomerase-independent chaperone function of cyclophilin ensures aggregation prevention of adenosine kinase both in vitro and under in vivo conditions. Biochemistry 43: 11862-11872.

562 31. Sen B, Venugopal V, Chakraborty A, Datta R, Dolai S, et al. (2007) Amino acid residues of
563 Leishmania donovani cyclophilin key to interaction with its adenosine kinase: biological
564 implications. Biochemistry 46: 7832-7843.
565 32. Alcolea PJ, Alonso A, Sanchez-Gorostiaga A, Moreno-Paz M, Gomez MJ, et al. (2009)
566 Genome-wide analysis reveals increased levels of transcripts related with infectivity in
567 peanut lectin non-agglutinated promastigotes of Leishmania infantum. Genomics 93:
568 551-564.
569 33. Yano M, Mori S, Niwa Y, Inoue M, Kido H (1997) Intrinsic nucleoside diphosphate kinase-
570 like activity as a novel function of 14-3-3 proteins. FEBS Lett 419: 244-248.
571 34. Silverman JM, Chan SK, Robinson DP, Dwyer DM, Nandan D, et al. (2008) Proteomic
572 analysis of the secretome of Leishmania donovani. Genome Biol 9: R35.
573 35. Alcolea PJ (2011) Análisis de los perfiles de expresión génica en los procesos de
574 diferenciación de Leishmania infantum mediante microarrays de ADN. E-Prints
575 Complutense: Universidad Complutense de Madrid. 292 p.
576 36. da Fonseca Pires S, Fialho LC, Jr., Silva SO, Melo MN, de Souza CC, et al. (2014)
577 Identification of virulence factors in Leishmania infantum strains by a proteomic
578 approach. J Proteome Res 13: 1860-1872.
579 37. Genestra M, Cysne-Finkelstein L, Leon L (2004) Protein kinase A activity is associated with
580 metacyclogenesis in Leishmania amazonensis. Cell Biochem Funct 22: 315-320.
581 38. Bhattacharya A, Biswas A, Das PK (2012) Identification of a protein kinase A regulatory
582 subunit from Leishmania having importance in metacyclogenesis through induction of
583 autophagy. Mol Microbiol 83: 548-564.
584 39. Gonzalez-Aseguinolaza G, Taladriz S, Marquet A, Larraga V (1999) Molecular cloning, cell
585 localization and binding affinity to DNA replication proteins of the p36/LACK protective
586 antigen from Leishmania infantum. Eur J Biochem 259: 909-916.
587 40. Alcolea PJ, Alonso A, Garcia-Tabares F, Torano A, Larraga V (2014) An Insight into the
588 proteome of Crithidia fasciculata choanomastigotes as a comparative approach to
589 axenic growth, peanut lectin agglutination and differentiation of Leishmania spp.
590 promastigotes. PLoS One 9: e113837.
591 41. Ramos I, Alonso A, Peris A, Marcen JM, Abengozar MA, et al. (2009) Antibiotic resistance
592 free plasmid DNA expressing LACK protein leads towards a protective Th1 response
593 against Leishmania infantum infection. Vaccine 27: 6695-6703.
594 42. Barrett MP, Mottram JC, Coombs GH (1999) Recent advances in identifying and validating
595 drug targets in trypanosomes and leishmanias. Trends Microbiol 7: 82-88.
596 43. Croft SL, Yardley V (2002) Chemotherapy of leishmaniasis. Curr Pharm Des 8: 319-342.
597 44. Verlinde CL, Hannaert V, Blonski C, Willson M, Perie JJ, et al. (2001) Glycolysis as a target
598 for the design of new anti-trypanosome drugs. Drug Resist Updat 4: 50-65.
599 45. Kushawaha PK, Gupta R, Tripathi CD, Khare P, Jaiswal AK, et al. (2012) Leishmania donovani
600 triose phosphate isomerase: a potential vaccine target against visceral leishmaniasis.
601 PLoS One 7: e45766.
602 46. Alcolea PJ, Alonso A, Gomez MJ, Sanchez-Gorostiaga A, Moreno-Paz M, et al. (2010)
603 Temperature increase prevails over acidification in gene expression modulation of
604 amastigote differentiation in Leishmania infantum. BMC Genomics 11: 31.
605 47. Guerra DG, Vertommen D, Fothergill-Gilmore LA, Opperdoes FR, Michels PA (2004)
606 Characterization of the cofactor-independent phosphoglycerate mutase from
607 Leishmania mexicana mexicana. Histidines that coordinate the two metal ions in the
608 active site show different susceptibilities to irreversible chemical modification. Eur J
609 Biochem 271: 1798-1810.
610 48. Fothergill-Gilmore LA, Watson HC (1989) The phosphoglycerate mutases. Adv Enzymol
611 Relat Areas Mol Biol 62: 227-313.
612 49. Fraser HI, Kvaratskhelia M, White MF (1999) The two analogous phosphoglycerate mutases
613 of Escherichia coli. FEBS Lett 455: 344-348.

50. Davis AJ, Perugini MA, Smith BJ, Stewart JD, Ilg T, et al. (2004) Properties of GDP-mannose pyrophosphorylase, a critical enzyme and drug target in Leishmania mexicana. J Biol Chem 279: 12462-12468.
51. Tetaud E, Fairlamb AH (1998) Cloning, expression and reconstitution of the trypanothione-dependent peroxidase system of Crithidia fasciculata. Mol Biochem Parasitol 96: 111-123.
52. Castro H, Sousa C, Santos M, Cordeiro-da-Silva A, Flohe L, et al. (2002) Complementary antioxidant defense by cytoplasmic and mitochondrial peroxiredoxins in Leishmania infantum. Free Radic Biol Med 33: 1552-1562.
53. Gordon S (2003) Alternative activation of macrophages. Nat Rev Immunol 3: 23-35.
54. Goerdt S, Politz O, Schledzewski K, Birk R, Gratchev A, et al. (1999) Alternative versus classical activation of macrophages. Pathobiology 67: 222-226.
55. Gaur U, Roberts SC, Dalvi RP, Corraliza I, Ullman B, et al. (2007) An effect of parasite-encoded arginase on the outcome of murine cutaneous leishmaniasis. J Immunol 179: 8446-8453.
56. Muleme HM, Reguera RM, Berard A, Azinwi R, Jia P, et al. (2009) Infection with arginase-deficient Leishmania major reveals a parasite number-dependent and cytokine-independent regulation of host cellular arginase activity and disease pathogenesis. J Immunol 183: 8068-8076.
57. Alcolea PJ, Alonso A, Gomez MJ, Postigo M, Molina R, et al. (2014) Stage-specific differential gene expression in Leishmania infantum: from the foregut of Phlebotomus perniciosus to the human phagocyte. BMC Genomics 15: 849.
58. Bates PA (2006) Housekeeping by Leishmania. Trends Parasitol 22: 447-448.
59. Depledge DP, Evans KJ, Ivens AC, Aziz N, Maroof A, et al. (2009) Comparative expression profiling of Leishmania: modulation in gene expression between species and in different host genetic backgrounds. PLoS Negl Trop Dis 3: e476.

Figure legends.

Fig 1. Growth curve of *L. amazonensis* promastigotes. Total protein samples were prepared and quantified at day 2 (early logarithmic phase), day 3 (mid logarithmic phase), day 5 (late logarithmic phase/early stationary phase) and day 7 (stationary phase).

Fig 2. Examples of 2DE of total protein extracts of *L. amazonensis* promastigotes. (A) Early logarithmic (day 2) and (B) stationary phase (day 7). IEF was performed in a non-linear 3-10 pH interval. (C) 3D density graphs of spots Lam2801, Lam3501, Lam6102 and Lam7004 obtained with PD Quest software.

Fig 3. Differential abundance of proteins involved in *L. amazonensis* metabolism. Constitutively expressed and differentially regulated proteins that participate in glycolysis, the Krebs cycle, amino acid metabolism and β-oxidation of fatty acids are depicted. Colour legend for up-regulation: green, day 2 (lag/early log); blue, day 3 (log); orange, day 5 (late log); red, day 7 (stat). The constitutively expressed proteins experimentally detected throughout the promastigote growth curve are highlighted in violet. Abbreviations not detailed in the text: ALD, fructose-1,6-bisphosphate aldolase; FMR, fumarase; MDH, malate dehydrogenase; PGK, phosphoglycerate kinase; PK, pyruvate kinase; SDH, succinate dehydrogenase.

Fig 4. Differential abundance of proteins involved in redox homeostasis. The FE-SOD participates in ROS processing providing hydrogen peroxide, which is then reduced by the TryP with the assistance of the TXN1, trypanithione and TryR. TryP differential expression pattern is complex through the promastigote growth curve of L. amazonensis. A light TryP variant is up-regulated in stationary phase promastigotes. A heavier TryP variant is down-regulated at day 3 and another one up-regulated simultaneously. Finally, a fourth variant is constitutively expressed during promastigote

growth. Colour legend for up-regulation: green, day 2 (lag/early log); blue, day 3 (log); orange, day 5 (late log); red, day 7 (stat). The constitutively expressed proteins experimentally detected throughout the promastigote growth curve are highlighted in violet.

Supplementary material.

S1 Fig. Scatter plot of differential protein abundance in *L. amazonensis* promastigotes.

S1 Table. Spot density values.

Table 1. Differential gene expression regulation in *L. amazonensis* promastigotes. The MW and pI values provided were estimated by the 2DE analysis software PD Quest. Theoretical values can be obtained from the *L. mexicana* LmxM genome databank within TriTrypDB by introducing the gene Ids. provided in this table.

Spot	TriTrypDB ID	Protein	MASCOT score ($p < 0.05$)	MW (KDa)	pI	Day3:Day2 ($p < 0.05$)	Day5:Day2 ($p < 0.05$)	Day7:Day2 ($p < 0.05$)
Lam 102	LmxM.34.4470	Hypothetical protein, conserved	300	23.74	3.3	0.51 (-1.96)	0.39 (-2.56)	0.56 (-1.78)
Lam1101	LmxM.04.0770/ 60	Unspecified product	96/89	23.16	4.0		0.5 (-2.00)	0.31 (-3.22)
Lam1103	LmxM.14.0190	Hypothetical protein, conserved	512	25.18	4.7	0.57 (-1.75)		
Lam1204	LmxM.36.3210	14-3-3 protein 1, putative	442	27.66	4.6		0.36 (-2.78)	
Lam1205	LmxM.08.1230	Beta tubulin	640	30.55	4.8			2.55
Lam1503	LmxM.25.0750	Protein phosphatase, putative	512	44.71	4.6	0.53 (-1.89)		0.56 (-1.78)
Lam1702	LmxM.13.0160	Protein kinase A regulatory subunit, putative	70	66.63	4.7			24.28
Lam2001	LmxM.15.0281/75	Ribonucleoprotein p18, mitochondrial precursor, putative	247/247	17.44	5.2		0.34 (-2.94)	
Lam2202	LmxM.13.0300	Unspecified product	206	27.99	5.1			40.22
Lam2304	LmxM.14.0310	Proteasome alpha 3 subunit	187	31.14	5.3			1.86
Lam2401	LmxM.25.1710	Pyruvate dehydrogenase E1 beta subunit, putative	133	38.28	5.2	0.27 (-3.7)	0.17 (-5.89)	
Lam2801	LmxM.32.0312/ 14/16	Heat shock protein 83-1	614/614/614	91.86	5.0	3.03		
Lam3102	LmxM.23.0040	Peroxidoxin	589	22.38	5.5		0.36 (-2.78)	
Lam3201	LmxM.34.1480	Arginase (ARG)	67	27.65	5.5		18.08	28.89
Lam3301	LmxM.34.1540	Rieske iron-sulfur protein, mitochondrial precursor, putative (RISP)	105	32.87	5.5		0.38 (-2.63)	
Lam3501	LmxM.28.2770/80	Heat-shock protein hsp70, putative	234/165	44.50	5.4			24.06
Lam3505	LmxM.07.0640	Hypothetical protein, conserved	320	40.57	5.5		0.09 (-11.1)	
Lam3601	LmxM.14.1160	Enolase	586	49.17	5.6		0.48 (-2.08)	0.49 (-2.04)
Lam3701	LmxM.36.2020/30	Chaperonin hsp60, mitochondrial precursor	820/356	67.83	5.3		0.01 (-100)	
Lam3704	LmxM.36.2030/20	Chaperonin hsp60 mitochondrial precursor	700	66.34	5.5		0.21 (-4.76)	0.49 (-2.04)
Lam3705	LmxM.36.6650	2,3-bisphosphoglycerate-independent phosphoglycerate mutase	304	68.99	5.5		60.01	
Lam3801	LmxM.28.2770/80	Heat-shock protein hsp70, putative	990/211	73.81	5.4		0.44 (-2.27)	
Lam3803	LmxM.29.2490/60/70	Heat shock 70-related protein 1, mitochondrial precursor, putative	874/727/726	76.87	5.5		0.32 (-3.12)	
Lam3901	LmxM.22.1540	Alanyl-tRNA synthetase, putative	376	112.48	5.6	1.83		
Lam4001	LmxM.23.0200	Endoribonuclease L-PSP (pb5), putative	360	12.93	5.7			1.76

Lam4002	LmxM.34.1300	Ubiquitin-conjugating enzyme E2, putative	135	12.16	5.5		0.46 (-2.17)	
Lam4401	LmxM.23.0110	Mannose-1-phosphate guanyltransferase (GDP-MP)	344	39.32	5.6		2.63	
Lam4403	LmxM.30.2250	3,2-trans-enoyl-CoA isomerase, mitochondrial precursor, putative	251	37.59	5.7	0.59 (-1.70)		
Lam5001	LmxM.15.1160/40	Tryparedoxin peroxidase	200/75	12.88	5.9			30.53
Lam5002	LmxM.20.1280	Calpain-like cysteine peptidase, Clan CA, family C2, putative	324	13.92	6.1		0.02 (-50.00)	0.01 (-100.00)
Lam5103	LmxM.15.1160/40	Tryparedoxin peroxidase	216/82	21.97	6.0	47.02		
Lam5302	LmxM.28.2740	Activated protein kinase C receptor (LACK)	510	32.08	6.1	0.51 (-1.96)	0.27 (-3.70)	0.25 (-4)
Lam5501	LmxM.06.0370	Glutamine synthetase, putative	262	41.01	5.9		0.38 (-2.63)	0.54 (-1.85)
Lam5502	LmxM.32.2300	UDP-glucose-4'-epimerase, putative	354	43.91	5.9		0.55 (-1.82)	
Lam5504	LmxM.06.0880	Acyl-coenzyme A dehydrogenase, putative	146	44.02	6.1			14.91
Lam5801	LmxM.30.0010	5-methyltetrahydropteroyltriglutamate-homocysteine methyltransferase, putative (MET6)	575	92.78	5.9	3.49		
Lam5804	LmxM.36.0180	Elongation factor 2	560	107.45	6.1	1.76	0.42 (-2.38)	0.41 (-2.43)
Lam5901	LmxM.36.0180	Elongation factor 2	449	107.63	6.0	2.35		
Lam6102	LmxM.15.1160/40	Tryparedoxin peroxidase	305/163	21.94	6.5	0.58 (-1.72)		
Lam6403	LmxM.36.4170	Oxidoreductase, putative	194	36.13	6.3		0.03 (-33.3)	
Lam6701	LmxM.34.3860	T-complex protein 1, eta subunit, putative	402	69.50	6.2		0.06(-16.67)	
Lam6702	LmxM.36.2660	Dihydrolipoamide acetyltransferase	128	55.74	6.3		0.45 (-2.22)	
Lam6703	LmxM.11.0630/20	Aminopeptidase, putative,metallo-peptidase, Clan MF, Family M17/aminopeptidase, putative	325/186	61.94	6.3	3.33		2.72
Lam6704	LmxM.31.3310	Dihydrolipoamide dehydrogenase	565	55.19	6.4			0.57 (-1.75)
Lam6801	LmxM.28.2770	Heat-shock protein hsp70, putative	190	73.71	6.2		0.31 (-3.22)	
Lam6806	LmxM.31.2951/50	Nucleoside diphosphate kinase b	553/553	88.79	6.8	0.09 (-11.1)		0.06 (-16.67)
Lam7003	LmxM.31.2951/50	Nucleoside diphosphate kinase b	544/544	13.19	7.5		0.31 (-3.22)	
Lam7004	LmxM.31.1820/30	Iron superoxide dismutase, putative	476/265	19.91	7.6	1.75		
Lam7603	LmxM.34.1380	Mitochondrial processing peptidase, beta subunit, putative, metallo-peptidase, Clan ME, family M16	522	52.84	7.0	40.36		
Lam7605	LmxM.34.1380	Mitochondrial processing peptidase, beta subunit, putative, metallo-peptidase, Clan ME, family M16	681	50.37	7.5	1.76		
Lam7701	LmxM.34.3860	T-complex protein 1, eta subunit, putative	427	63.99	6.8		0.4 (-2.5)	0.52 (-1.92)
Lam7702	LmxM.36.0180	Elongation factor 2	300	60.30	6.9	3.34		
Lam7703	LmxM.36.0070	Stress-inducible protein STI1 homolog	318	65.49	7.4	0.5 (-2.00)	0.24 (-4.17)	0.59 (-1.70)

Lam7801	LmxM.18.0510	Aconitase, putative	502	103.24	7.0		0.43 (-2.32)	
Lam8003	LmxM.06.0120	Cyclophilin	321	13.18	9.2	0.51 (-1.96)	0.48 (-2.08)	
Lam8005	LmxM.26.1380	Prefoldin-like protein/Cyclophilin, putative	125/106	21.02	9.5	30.56		
Lam8101	LmxM.24.0850	Triose phosphate isomerase	621	23.26	9.1	0.44 (-2.27)	0.43 (-2.32)	
Lam8102	LmxM.36.0070	Stress-inducible protein STI1 homolog	347	25.49	9.4		0.43 (-2.32)	
Lam8201	LmxM.24.1980	Hypothetical protein, conserved	404	30.12	9.2			15.15
Lam8501	LmxM.31.0840	Hypothetical protein, conserved	188	42.92	8.2		0.36 (-2.78)	0.33 (-3.03)
Lam8701	LmxM.25.1120	Aldehyde dehydrogenase, mitochondrial precursor	497	54.99	8.0			1.77
Lam8703	LmxM.07.0340	ATP-dependent DEAD/H RNA helicase, putative	201	67.09	9.4	6.04		
Lam8706	LmxM.03.0200/24.0770	Delta1-pyrroline-5-carboxylate dehydrogenase, putative/Malic enzyme, putative	181/163	59.28	9.1	20.4		

Table 2. Constitutively expressed proteins in L. amazonensis promastigotes. The MW and pI values provided were estimated by the 2DE analysis software PD Quest. Theoretical values can be obtained from the *L. mexicana* LmxM genome databank within TriTrypDB by introducing the gene Ids. provided in this table.

Spot	TriTrypDB ID	Protein	MASCOT score ($p < 0.05$)	MW (KDa)	pI
Lam1601	ACY70938 (NCBI Id.)	Soluble promastigote surface antigen PSA-31S	221	74.38	4.4
Lam2502	LmxM.32.0312/14/16	Heat shock protein 83-1	288/288/288	61.34	5.1
Lam2601	LmxM.36.6940	Protein disulfide isomerase	395	73.85	5.5
Lam2803	LmxM.28.1200	Glucose-regulated protein 78, putative	611	105.47	5.2
Lam2804	LmxM.36.1370	Transitional endoplasmic reticulum ATPase, putative, valosin-containing protein homolog	185	147.73	5.7
Lam3001	LmxM.08_29.1160	Tryparedoxin 1, putative (TXN1)	228	13.20	5.4
Lam3802	LmxM.29.1760/50	Paraflagellar rod protein 1D, putative	312/312	127.12	5.4
Lam4601	LmxM.32.2540	Carboxypeptidase, putative,metallo-peptidase, Clan MA(E), Family M32	457	79.14	5.7
Lam4801	LmxM.26.1570	Thimet oligopeptidase, putative,metallo-peptidase, Clan MA(E), Family M3	247	98.15	5.7
Lam4803	LmxM.28.2770/20	Heat-shock protein HSP70, putative	199	97.64	5.8
Lam5503	LmxM.01.0770	Unspecified product	315	73.92	6.0
Lam5506	LmxM.36.2950	Succinyl-CoA ligase (GDP-forming) beta chain, putative	748	54.02	6.2
Lam5702	LmxM.27.1260	T-complex protein 1, beta subunit, putative	279	80.04	6.1
Lam5803	LmxM.36.0180	Elongation factor 2	136	124.23	6.0
Lam6402	LmxM.25.1610	Hypothetical protein, conserved	79	62.25	6.4
Lam6705	LmxM.27.1220	Hypothetical protein, conserved	145	78.46	6.6
Lam7503	LmxM.10.0290	Isocitrate dehydrogenase (NADP), mitochondrial precursor, putative	283	65.21	7.5
Lam7602	LmxM.18.0670	Citrate synthase, putative	273/270	74.91	6.8
Lam7604	LmxM.21.0340	Mitochondrial processing peptidase alpha subunit, putative,metallo-peptidase, Clan ME, Family M16	223	74.26	7.2
Lam8001	LmxM.15.1160/40	Tryparedoxin peroxidase	248/102	22.46	8.5
Lam8103	LmxM.21.0850	Xanthine phosphoribosyltransferase	319	24.12	9.4
Lam8203	LmxM.36.5120/10	40S ribosomal protein SA, putative	354/255	34.03	9.4
Lam8403	LmxM.36.1260	Fructose-1,6-bisphosphate aldolase	458	66.15	9.5
Lam8601	LmxM.32.2340	Succinyl-CoA:3-ketoacid coenzyme A transferase, mitochondrial precursor, putative	712	68.41	8.2
Lam9201	LmxM.02.0460	Voltage-dependent anion-selective channel, putative (VDAC)	298	36.34	9.5

Lam9301	LmxM.25.2130/40	Succinyl-CoA synthetase alpha subunit, putative	319/319	47.70	9.5
Lam9401	LmxM.29.2980	Glyceraldehyde-3-phosphate dehydrogenase, glycosomal	458	48.53	9.5

Table 3. Remarkable examples of protein variants. Comparison of experimental (Exp) and predicted theoretical (P) MW and pI.

TriTryp Id.	Protein	^{Exp}MW	^{P}MW	^{Exp}pI	^{P}pI
LmxM.15.1160	TryP	12.9	22.2	8.5	6.7
LmxM.15.1160	TryP	22.0	22.2	6.0	6.7
LmxM.15.1160	TryP	21.9	22.2	6.5	6.7
LmxM.28.2770	HSP70	44.5	71.2	5.4	5.2
LmxM.28.2770	HSP70	73.8	71.2	5.4	5.2
LmxM.28.2770	HSP70	73.7	71.2	6.2	5.2
LmxM.28.2770	HSP70	97.6	71.2	5.8	5.2
LmxM.29.2490	HSP70-rel1	76.9	72.5	5.5	5.7
LmxM.31.2951	NDKb	88.79	16.7	6.8	7.5
LmxM.31.2951	NDKb	13.2	16.7	7.5	7.5
LmxM.34.1380	M16 peptidase	52.8	54.6	7.0	7.1
LmxM.34.1380	M16 peptidase	50.4	54.6	7.5	7.1
LmxM.36.0180	EF2	107.4	94.1	6.1	6.0
LmxM.36.0180	EF2	107.6	94.1	6.0	6.0
LmxM.36.0180	EF2	60.3	94.1	6.9	6.0

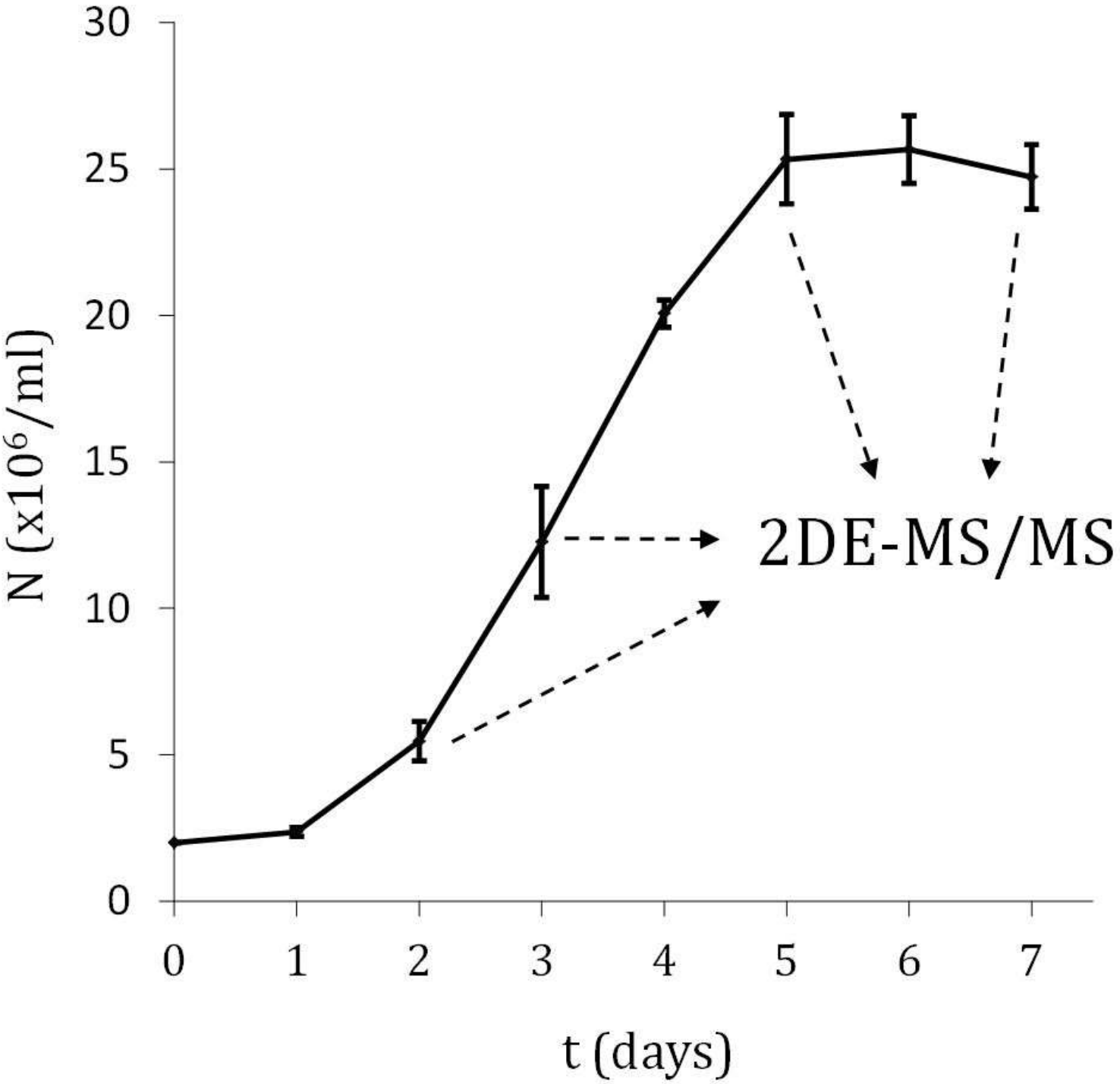
30
25
20
15
10
5
0
N (x10^6/ml)
0
1
2
3
4
5
6
7
t (days)
2DE-MS/MS

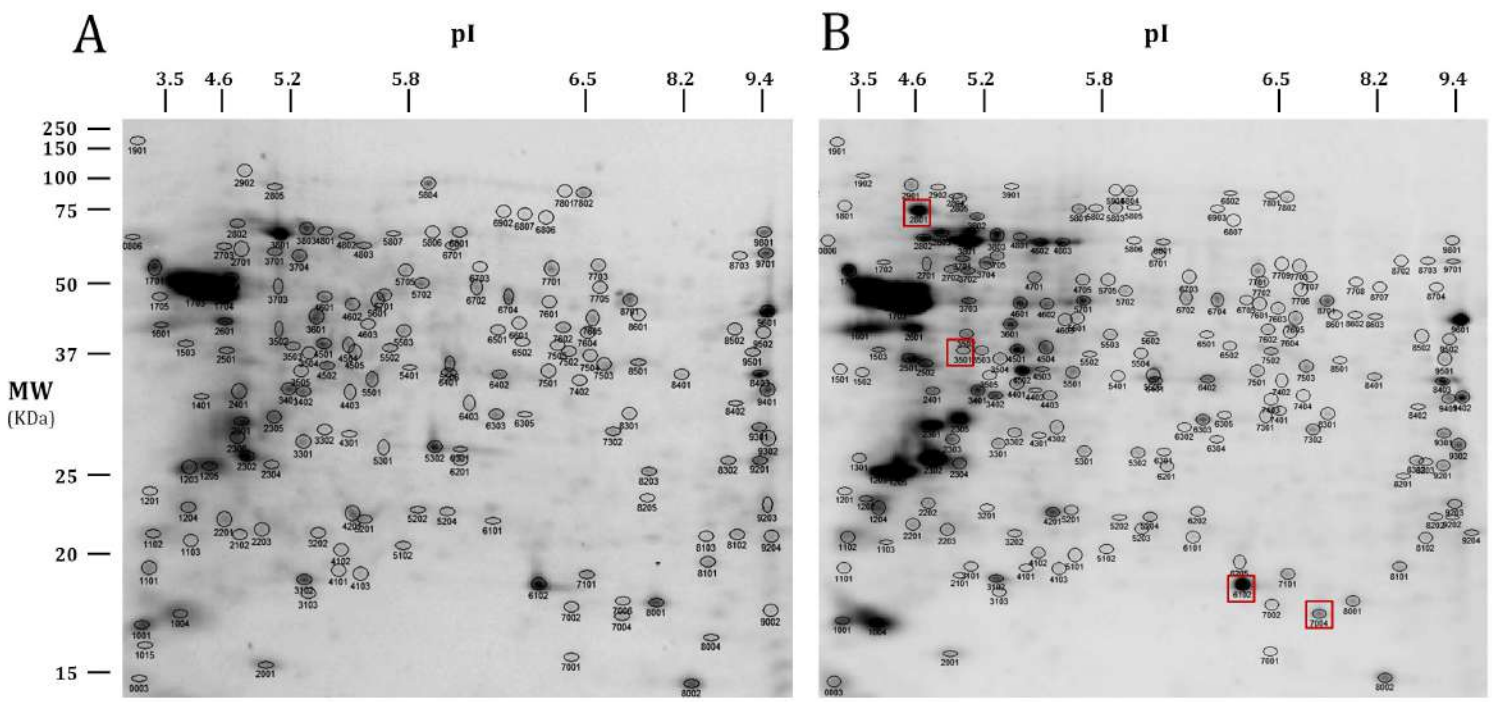

C

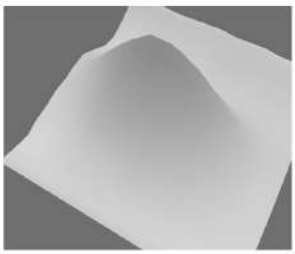

Lam2801 (hsp83-1)

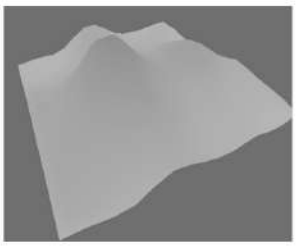

Lam3501 (hsp70)

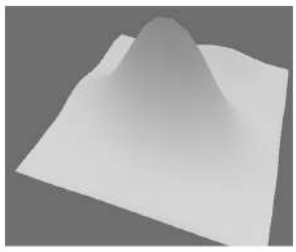

Lam6102 (TryP)

Lam7004 (Fe-SOD)

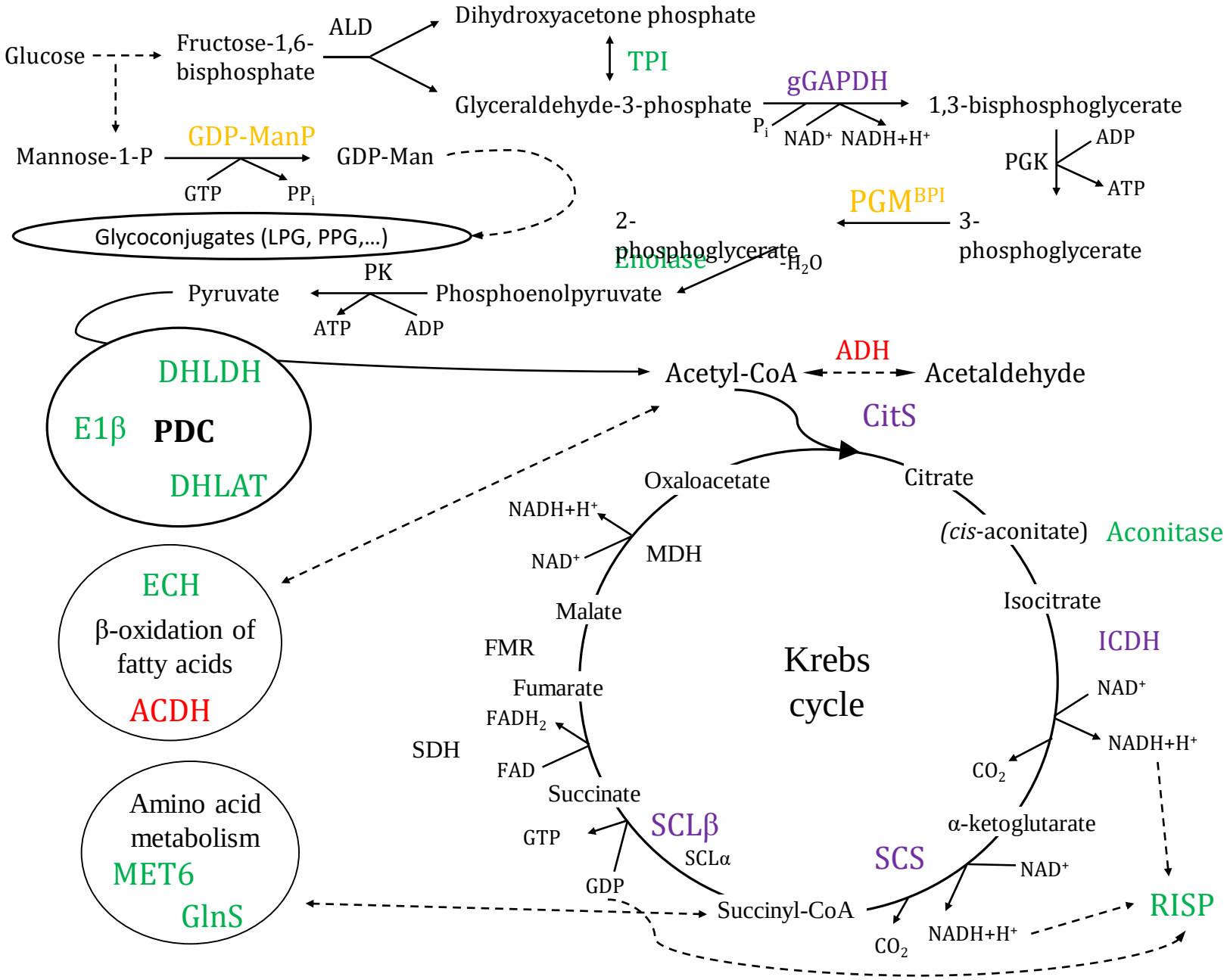
Glucose
Fructose-1,6-bisphosphate
ALD
Dihydroxyacetone phosphate
TPI
Glyceraldehyde-3-phosphate
gGAPDH
Pi
NAD+ NADH+H+
1,3-bisphosphoglycerate
PGK
ADP
ATP
Mannose-1-P
GDP-ManP
GTP
PPi
GDP-Man
Glycoconjugates (LPG, PPG,...)
PGMBPI
3-phosphoglycerate
2-phosphoglycerate
Enolase
-H2O
PK
Pyruvate
Phosphoenolpyruvate
ATP
ADP
DHLDH
E1β
PDC
DHLAT
Acetyl-CoA
ADH
Acetaldehyde
CitS
Oxaloacetate
Citrate
NADH+H+
NAD+
MDH
(cis-aconitate)
Aconitase
Malate
Isocitrate
FMR
ICDH
Fumarate
Krebs cycle
NAD+
FADH2
NADH+H+
SDH
FAD
CO2
Succinate
α-ketoglutarate
ECH
β-oxidation of fatty acids
ACDH
SCLβ
GTP
SCS
NAD+
SCLα
GDP
Succinyl-CoA
RISP
CO2
NADH+H+
Amino acid metabolism
MET6
GlnS

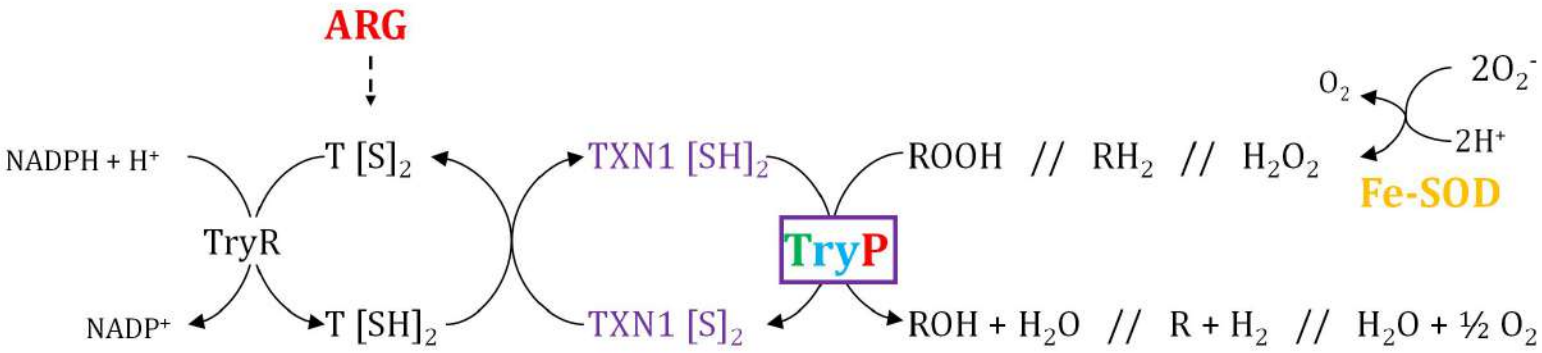
ARG
NADPH + H+
T [S]2
TryR
NADP+
T [SH]2
TXN1 [SH]2
TXN1 [S]2
TryP
ROOH // RH2 // H2O2
ROH + H2O // R + H2 // H2O + ½ O2
O2
2O2-
2H+
Fe-SOD

Table 1. Differential gene expression regulation in *L. amazonensis* promastigotes. The MW and pI values provided were estimated by the 2DE analysis software PD Quest. Theoretical values can be obtained from the *L. mexicana* LmxM genome databank within TriTrypDB by introducing the gene Ids. provided in this table.

Spot	TriTrypDB ID	Protein	MASCOT score ($p < 0.05$)	MW (KDa)	pI	Day3:Day2 ($p < 0.05$)	Day5:Day2 ($p < 0.05$)	Day7:Day2 ($p < 0.05$)
Lam 102	LmxM.34.4470	Hypothetical protein, conserved	300	23.74	3.3	0.51 (-1.96)	0.39 (-2.56)	0.56 (-1.78)
Lam1101	LmxM.04.0770/ 60	Unspecified product	96/89	23.16	4.0		0.5 (-2.00)	0.31 (-3.22)
Lam1103	LmxM.14.0190	Hypothetical protein, conserved	512	25.18	4.7	0.57 (-1.75)		
Lam1204	LmxM.36.3210	14-3-3 protein 1, putative	442	27.66	4.6		0.36 (-2.78)	
Lam1205	LmxM.08.1230	Beta tubulin	640	30.55	4.8			2.55
Lam1503	LmxM.25.0750	Protein phosphatase, putative	512	44.71	4.6	0.53 (-1.89)		0.56 (-1.78)
Lam1702	LmxM.13.0160	Protein kinase A regulatory subunit, putative	70	66.63	4.7			24.28
Lam2001	LmxM.15.0281/75	Ribonucleoprotein p18, mitochondrial precursor, putative	247/247	17.44	5.2		0.34 (-2.94)	
Lam2202	LmxM.13.0300	Unspecified product	206	27.99	5.1			40.22
Lam2304	LmxM.14.0310	Proteasome alpha 3 subunit	187	31.14	5.3			1.86
Lam2401	LmxM.25.1710	Pyruvate dehydrogenase E1 beta subunit, putative	133	38.28	5.2	0.27 (-3.7)	0.17 (-5.89)	
Lam2801	LmxM.32.0312/ 14/16	Heat shock protein 83-1	614/614/614	91.86	5.0	3.03		
Lam3102	LmxM.23.0040	Peroxidoxin	589	22.38	5.5		0.36 (-2.78)	
Lam3201	LmxM.34.1480	Arginase (ARG)	67	27.65	5.5		18.08	28.89
Lam3301	LmxM.34.1540	Rieske iron-sulfur protein, mitochondrial precursor, putative (RISP)	105	32.87	5.5		0.38 (-2.63)	
Lam3501	LmxM.28.2770/80	Heat-shock protein hsp70, putative	234/165	44.50	5.4			24.06
Lam3505	LmxM.07.0640	Hypothetical protein, conserved	320	40.57	5.5		0.09 (-11.1)	
Lam3601	LmxM.14.1160	Enolase	586	49.17	5.6		0.48 (-2.08)	0.49 (-2.04)
Lam3701	LmxM.36.2020/30	Chaperonin hsp60, mitochondrial precursor	820/356	67.83	5.3		0.01 (-100)	
Lam3704	LmxM.36.2030/20	Chaperonin hsp60 mitochondrial precursor	700	66.34	5.5		0.21 (-4.76)	0.49 (-2.04)
Lam3705	LmxM.36.6650	2,3-bisphosphoglycerate-independent phosphoglycerate mutase	304	68.99	5.5		60.01	
Lam3801	LmxM.28.2770/80	Heat-shock protein hsp70, putative	990/211	73.81	5.4		0.44 (-2.27)	
Lam3803	LmxM.29.2490/60/70	Heat shock 70-related protein 1, mitochondrial precursor, putative	874/727/726	76.87	5.5		0.32 (-3.12)	
Lam3901	LmxM.22.1540	Alanyl-tRNA synthetase, putative	376	112.48	5.6	1.83		
Lam4001	LmxM.23.0200	Endoribonuclease L-PSP (pb5), putative	360	12.93	5.7			1.76

Lam4002	LmxM.34.1300	Ubiquitin-conjugating enzyme E2, putative	135	12.16	5.5		0.46 (-2.17)	
Lam4401	LmxM.23.0110	Mannose-1-phosphate guanyltransferase (GDP-MP)	344	39.32	5.6		2.63	
Lam4403	LmxM.30.2250	3,2-trans-enoyl-CoA isomerase, mitochondrial precursor, putative	251	37.59	5.7	0.59 (-1.70)		
Lam5001	LmxM.15.1160/40	Tryparedoxin peroxidase	200/75	12.88	5.9			30.53
Lam5002	LmxM.20.1280	Calpain-like cysteine peptidase, Clan CA, family C2, putative	324	13.92	6.1		0.02 (-50.00)	0.01 (-100.00)
Lam5103	LmxM.15.1160/40	Tryparedoxin peroxidase	216/82	21.97	6.0	47.02		
Lam5302	LmxM.28.2740	Activated protein kinase C receptor (LACK)	510	32.08	6.1	0.51 (-1.96)	0.27 (-3.70)	0.25 (-4)
Lam5501	LmxM.06.0370	Glutamine synthetase, putative	262	41.01	5.9		0.38 (-2.63)	0.54 (-1.85)
Lam5502	LmxM.32.2300	UDP-glucose-4'-epimerase, putative	354	43.91	5.9		0.55 (-1.82)	
Lam5504	LmxM.06.0880	Acyl-coenzyme A dehydrogenase, putative	146	44.02	6.1			14.91
Lam5801	LmxM.30.0010	5-methyltetrahydropteroyltriglutamate-homocysteine methyltransferase, putative (MET6)	575	92.78	5.9	3.49		
Lam5804	LmxM.36.0180	Elongation factor 2	560	107.45	6.1	1.76	0.42 (-2.38)	0.41 (-2.43)
Lam5901	LmxM.36.0180	Elongation factor 2	449	107.63	6.0	2.35		
Lam6102	LmxM.15.1160/40	Tryparedoxin peroxidase	305/163	21.94	6.5	0.58 (-1.72)		
Lam6403	LmxM.36.4170	Oxidoreductase, putative	194	36.13	6.3		0.03 (-33.3)	
Lam6701	LmxM.34.3860	T-complex protein 1, eta subunit, putative	402	69.50	6.2		0.06(-16.67)	
Lam6702	LmxM.36.2660	Dihydrolipoamide acetyltransferase	128	55.74	6.3		0.45 (-2.22)	
Lam6703	LmxM.11.0630/20	Aminopeptidase, putative,metallo-peptidase, Clan MF, Family M17/aminopeptidase, putative	325/186	61.94	6.3	3.33		2.72
Lam6704	LmxM.31.3310	Dihydrolipoamide dehydrogenase	565	55.19	6.4			0.57 (-1.75)
Lam6801	LmxM.28.2770	Heat-shock protein hsp70, putative	190	73.71	6.2		0.31 (-3.22)	
Lam6806	LmxM.31.2951/50	Nucleoside diphosphate kinase b	553/553	88.79	6.8	0.09 (-11.1)		0.06 (-16.67)
Lam7003	LmxM.31.2951/50	Nucleoside diphosphate kinase b	544/544	13.19	7.5		0.31 (-3.22)	
Lam7004	LmxM.31.1820/30	Iron superoxide dismutase, putative	476/265	19.91	7.6	1.75		
Lam7603	LmxM.34.1380	Mitochondrial processing peptidase, beta subunit, putative, metallo-peptidase, Clan ME, family M16	522	52.84	7.0	40.36		
Lam7605	LmxM.34.1380	Mitochondrial processing peptidase, beta subunit, putative, metallo-peptidase, Clan ME, family M16	681	50.37	7.5	1.76		
Lam7701	LmxM.34.3860	T-complex protein 1, eta subunit, putative	427	63.99	6.8		0.4 (-2.5)	0.52 (-1.92)
Lam7702	LmxM.36.0180	Elongation factor 2	300	60.30	6.9	3.34		
Lam7703	LmxM.36.0070	Stress-inducible protein STI1 homolog	318	65.49	7.4	0.5 (-2.00)	0.24 (-4.17)	0.59 (-1.70)

Lam7801	LmxM.18.0510	Aconitase, putative	502	103.24	7.0		0.43 (-2.32)	
Lam8003	LmxM.06.0120	Cyclophilin	321	13.18	9.2	0.51 (-1.96)	0.48 (-2.08)	
Lam8005	LmxM.26.1380	Prefoldin-like protein/Cyclophilin, putative	125/106	21.02	9.5	30.56		
Lam8101	LmxM.24.0850	Triose phosphate isomerase	621	23.26	9.1	0.44 (-2.27)	0.43 (-2.32)	
Lam8102	LmxM.36.0070	Stress-inducible protein STI1 homolog	347	25.49	9.4		0.43 (-2.32)	
Lam8201	LmxM.24.1980	Hypothetical protein, conserved	404	30.12	9.2			15.15
Lam8501	LmxM.31.0840	Hypothetical protein, conserved	188	42.92	8.2		0.36 (-2.78)	0.33 (-3.03)
Lam8701	LmxM.25.1120	Aldehyde dehydrogenase, mitochondrial precursor	497	54.99	8.0			1.77
Lam8703	LmxM.07.0340	ATP-dependent DEAD/H RNA helicase, putative	201	67.09	9.4	6.04		
Lam8706	LmxM.03.0200/24.0770	Delta1-pyrroline-5-carboxylate dehydrogenase, putative/Malic enzyme, putative	181/163	59.28	9.1	20.4		

Table 2. Constitutively expressed proteins in L. amazonensis promastigotes. The MW and pI values provided were estimated by the 2DE analysis software PD Quest. Theoretical values can be obtained from the *L. mexicana* LmxM genome databank within TriTrypDB by introducing the gene Ids. provided in this table.

Spot	TriTrypDB ID	Protein	MASCOT score ($p < 0.05$)	MW (KDa)	pI
Lam1601	ACY70938 (NCBI Id.)	Soluble promastigote surface antigen PSA-31S	221	74.38	4.4
Lam2502	LmxM.32.0312/14/16	Heat shock protein 83-1	288/288/288	61.34	5.1
Lam2601	LmxM.36.6940	Protein disulfide isomerase	395	73.85	5.5
Lam2803	LmxM.28.1200	Glucose-regulated protein 78, putative	611	105.47	5.2
Lam2804	LmxM.36.1370	Transitional endoplasmic reticulum ATPase, putative, valosin-containing protein homolog	185	147.73	5.7
Lam3001	LmxM.08_29.1160	Tryparedoxin 1, putative (TXN1)	228	13.20	5.4
Lam3802	LmxM.29.1760/50	Paraflagellar rod protein 1D, putative	312/312	127.12	5.4
Lam4601	LmxM.32.2540	Carboxypeptidase, putative,metallo-peptidase, Clan MA(E), Family M32	457	79.14	5.7
Lam4801	LmxM.26.1570	Thimet oligopeptidase, putative,metallo-peptidase, Clan MA(E), Family M3	247	98.15	5.7
Lam4803	LmxM.28.2770/20	Heat-shock protein HSP70, putative	199	97.64	5.8
Lam5503	LmxM.01.0770	Unspecified product	315	73.92	6.0
Lam5506	LmxM.36.2950	Succinyl-CoA ligase (GDP-forming) beta chain, putative	748	54.02	6.2
Lam5702	LmxM.27.1260	T-complex protein 1, beta subunit, putative	279	80.04	6.1
Lam5803	LmxM.36.0180	Elongation factor 2	136	124.23	6.0
Lam6402	LmxM.25.1610	Hypothetical protein, conserved	79	62.25	6.4
Lam6705	LmxM.27.1220	Hypothetical protein, conserved	145	78.46	6.6
Lam7503	LmxM.10.0290	Isocitrate dehydrogenase (NADP), mitochondrial precursor, putative	283	65.21	7.5
Lam7602	LmxM.18.0670	Citrate synthase, putative	273/270	74.91	6.8
Lam7604	LmxM.21.0340	Mitochondrial processing peptidase alpha subunit, putative,metallo-peptidase, Clan ME, Family M16	223	74.26	7.2
Lam8001	LmxM.15.1160/40	Tryparedoxin peroxidase	248/102	22.46	8.5
Lam8103	LmxM.21.0850	Xanthine phosphoribosyltransferase	319	24.12	9.4
Lam8203	LmxM.36.5120/10	40S ribosomal protein SA, putative	354/255	34.03	9.4
Lam8403	LmxM.36.1260	Fructose-1,6-bisphosphate aldolase	458	66.15	9.5
Lam8601	LmxM.32.2340	Succinyl-CoA:3-ketoacid coenzyme A transferase, mitochondrial precursor, putative	712	68.41	8.2
Lam9201	LmxM.02.0460	Voltage-dependent anion-selective channel, putative (VDAC)	298	36.34	9.5

Lam9301	LmxM.25.2130/40	Succinyl-CoA synthetase alpha subunit, putative	319/319	47.70	9.5
Lam9401	LmxM.29.2980	Glyceraldehyde-3-phosphate dehydrogenase, glycosomal	458	48.53	9.5

Table 3. Remarkable examples of protein variants. Comparison of experimental (Exp) and predicted theoretical (P) MW and pI.

TriTryp Id.	Protein	^{Exp}MW	^{P}MW	^{Exp}pI	^{P}pI
LmxM.15.1160	TryP	12.9	22.2	8.5	6.7
LmxM.15.1160	TryP	22.0	22.2	6.0	6.7
LmxM.15.1160	TryP	21.9	22.2	6.5	6.7
LmxM.28.2770	HSP70	44.5	71.2	5.4	5.2
LmxM.28.2770	HSP70	73.8	71.2	5.4	5.2
LmxM.28.2770	HSP70	73.7	71.2	6.2	5.2
LmxM.28.2770	HSP70	97.6	71.2	5.8	5.2
LmxM.29.2490	HSP70-rel1	76.9	72.5	5.5	5.7
LmxM.31.2951	NDKb	88.79	16.7	6.8	7.5
LmxM.31.2951	NDKb	13.2	16.7	7.5	7.5
LmxM.34.1380	M16 peptidase	52.8	54.6	7.0	7.1
LmxM.34.1380	M16 peptidase	50.4	54.6	7.5	7.1
LmxM.36.0180	EF2	107.4	94.1	6.1	6.0
LmxM.36.0180	EF2	107.6	94.1	6.0	6.0
LmxM.36.0180	EF2	60.3	94.1	6.9	6.0

S1 Fig. Scatter plot of differential protein abundance in *L. amazonensis* promastigotes.
Three biological replicates of the experiment were considered. Day 7 vs. Day 2.

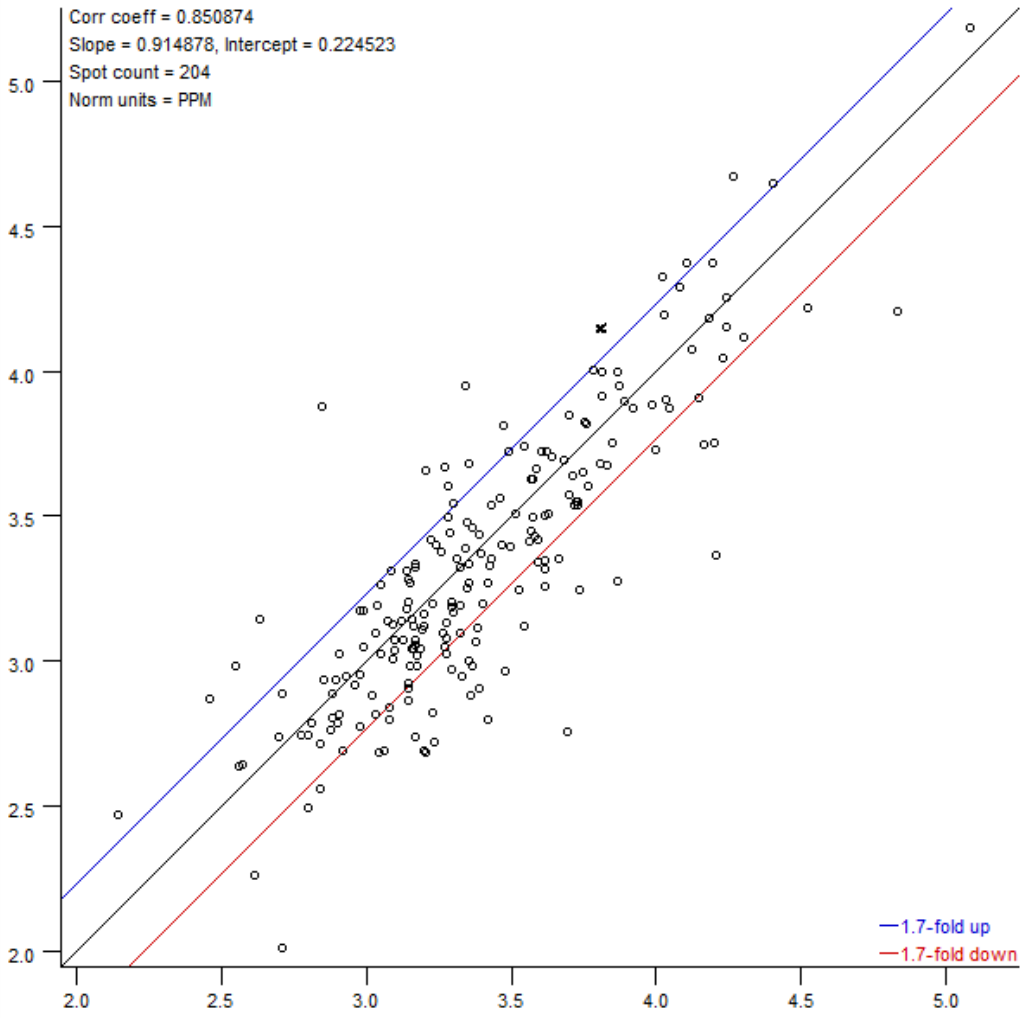

S1 Table. Spot density values.

Quantitation Table

SSP	d2r1	d2r2	d2r3	d3r1	d3r2	d3r3	d5r1
101	16287.2	14311.8	16532.4	30728.9	32524.8	9239.9	26247.3
102	5129.9	5611.3	4934.9	2553.8	2669.6	2723.5	2038.8
401	4813.5	1880.2	2596.1	7131.7	5465.6	975.6	4888.2
501					764.6		
601	13475.4	9677.1	13067.3	26148.8	23428.6	6317.0	20471.0
602					853.5		
603							
604							
701	3201.0		2113.2		1102.5		2136.6
702			4523.8		2708.3	9540.8	5276.8
703		8410.7	2299.1		3708.2		
801	11105.1	9020.2	11723.7	18980.9	14835.7	7237.4	12915.7
802	1606.4	2496.6	2250.5	3712.4	2768.2	1002.4	4817.5
803		2147.7			1574.2		
804	1856.2			739.7	748.7		
805		748.3					8678.6
806	10193.9	9630.8	27723.0	9114.2	2328.3	2148.6	60139.5
901	1404.7	1388.0	1378.2	2799.8	1830.0	503.2	3590.3
902		1643.9	847.4	1908.4		1393.1	
903				1227.6		419.5	
905	485.6	430.6	968.1			54.6	654.3
1001	8691.6	11741.5	8503.4	8323.3	6742.1	9054.7	3500.1
1002		15264.6	15209.5	5682.3	1142.5		1952.4
1003		2048.2					
1004	29090.1	11855.4	35042.8	8609.2	27488.0	11688.3	21282.9
1008		19892.6		4618.6			
1009	1046.1				1411.7		
1010	15988.2						
1011							
1012							
1013							
1014							
1015	1387.8			4307.3			
1101	3212.9	2765.3	3105.6	1948.0	2339.3	3075.3	1093.3
1102	9078.8	3975.5			2124.5		3996.8
1103	1597.8	2350.0	1909.7	921.0	1307.6		1421.6
1104							
1201	927.4	1259.7		1142.3		1682.6	
1202					1555.5		
1203	6764.4	8666.4		5219.0	23131.8	3672.9	5937.3
1204	4472.8	7296.6	5503.1	4545.6	5058.4	5930.1	3585.8
1205	16808.8	13588.8	25051.0	6916.1	14283.1	16878.1	18220.2
1301							1436.2
1302				3119.0			

1401	2019.0	1782.6					
1501							
1502		1378.7			1731.5		
1503	1934.8	1738.8	2014.8	965.7	973.8	1065.4	498.7
1601	12579.3	12769.1	12853.0	12236.8	4261.3	10088.5	10182.9
1602				1919.1			
1701	15698.1	13071.5	22289.0	12210.7	11975.4	19459.9	13562.4
1702	124.2	103.0		179.4	142.1	165.5	
1703	132386.7	71521.5	160322.4	182022.0	177814.9	240752.0	
1704	44931.3	96952.3	117200.6				65748.9
1705	919.7			7151.0			1795.4
1706							
1707		68249.8					
1801				2417.6		2673.5	
1802					5642.3	1440.7	
1803			2240.3		1924.1		
1901	795.1	1947.0	1424.8	606.2		1060.3	
1902				2384.6	1461.4	2662.7	
2001	7158.9	3992.9	5921.0	2171.2	4057.4	3862.2	2864.2
2002	2084.1	1662.5			1010.1		
2101						1466.6	
2102	1699.4						
2201	2281.5	1501.3					
2202							
2203	2622.6	4906.0	3684.2		2162.1	5311.2	4602.9
2301	10364.7	3979.6	7655.3		5082.9	5255.9	9730.6
2302	11417.8	8398.3	11742.7		6342.5	6760.6	14129.6
2303		1498.6	1637.1	49872.8		2041.1	
2304	7621.1	4518.0	6044.0		5803.6	4406.7	6133.9
2305	8633.5	4363.0	6135.7	6213.0	3246.4	2962.8	7397.3
2306	6185.1	8780.6		31485.2	2576.9		
2307			1667.0	2591.4			
2401	6987.4	2703.9	6592.2	929.2		2024.8	
2501	3605.1	6414.7	3125.6	10040.6	7145.8	3130.4	10905.9
2502	3562.2	4821.9	28054.6	7665.0	3565.8	6251.2	5131.1
2601	7494.0	7093.2	10464.5	4816.8	6246.8	5371.3	3579.4
2602						2044.0	
2701	919.0		2992.3			1639.2	20709.4
2702		1585.5		757.5	983.9	815.2	
2703	866.5	839.5	1915.0	185.5	1202.0		5917.0
2704	12872.5						
2801		5069.9	3328.6	12492.8	12322.4	13321.6	4074.4
2802	4922.8	1582.9	3251.1	1994.6	6028.9	6766.0	2016.6
2803	14225.8	17521.0	10495.4	11740.3	9415.8	10235.3	9246.4
2804		1705.1			1790.2		
2805	1591.6		2164.3	1870.7	2886.0	2153.9	
2806						2991.6	

2901		1132.7	1633.4	2438.6	1739.6	2870.5	
2902	589.5	1780.4	1328.0	2686.0	1237.0	2763.7	455.6
3001	2986.3	24715.0	19426.1	1624.6	2015.8	2545.2	2008.4
3002	1966.9		1226.1		1397.3		
3101							11957.6
3102	6568.9	6616.2	7844.6	2053.5	7395.0	5570.6	2986.0
3103	2237.8	2290.8			2831.3		815.5
3104							5458.6
3201	137.2	141.0					3966.9
3202	2923.5	2012.4					
3301	2141.5	1687.9	1655.9		4153.8	2045.1	874.8
3302	804.3						755.1
3303					1404.4		
3401	4444.1	3040.0	4108.1	7932.3	2597.5	4844.9	3601.2
3402	3003.2	3015.0	2093.2		5452.5	2839.2	3078.3
3501	152.3	201.6	194.8	131.7		220.9	
3502	5571.1	3426.9	3322.5	981.3	8155.7	1741.4	
3503	2421.4	1137.0	2139.0	1085.5		956.0	13262.7
3504	469.6	1129.2			2520.3	1154.3	14847.4
3505	419.8	617.2	187.6		417.4	458.5	
3601	6370.3	5865.6	5260.6	12339.4	2764.3	7896.5	1985.1
3602				1389.5	4238.1	1653.4	
3701	2585.9	1825.5	2851.7	287.4		2557.0	
3702		1382.9	1584.5	1572.2	2251.4	2471.2	586.1
3703	4653.7	2778.5		532.9	17581.4	1356.7	
3704	3936.5	4978.2	4992.1	3277.2	1962.2	3699.2	
3705					2480.9		1198.7
3706							
3707					3091.9		
3708					15140.7		
3801	13809.4	19389.0	19470.3	14575.4	11465.5	19074.7	11319.9
3802	1352.0	1216.9	2600.9	3160.4	1569.0	6101.4	1017.8
3803	9187.8	10701.3	13582.6		3216.5	8727.9	
3901		974.5		1290.5	2037.1	2027.9	
4001	6298.5	6879.1	6299.0		5947.9	7375.3	3955.3
4002	2440.7	2089.9	1432.1		1429.1	1467.6	683.1
4101	1005.8	1156.6					
4102	684.8	1017.2				1287.7	27312.8
4103	1392.5	1268.0		1979.0			
4201	4053.2	7727.4	7422.3	1703.2	4478.6	6163.2	4627.8
4202							
4301	1123.3						
4302		1423.8					
4303							
4304							
4401		428.1				975.0	1105.1
4402						787.3	

4403	1407.6	1683.6	1156.2	720.9	714.1	1076.3	740.2
4501	3829.9	3907.8	3909.0	5386.7	2164.5	2955.0	31116.7
4502	2325.8	1384.0	1883.6	1262.4	2319.2	2697.8	2882.4
4503		1478.7		574.0			666.8
4504	1715.5	1963.3	2046.0	2503.3			20449.1
4505	1211.7					486.8	
4506							20863.7
4601	2690.3	5902.3	6453.4	4277.1	4542.7	5393.2	4827.1
4602	1852.6	3666.4	5720.7	6392.5		4704.2	
4603	696.1			3364.5			
4604							
4701		705.0				1434.3	655.7
4702		5515.0	6179.6		9160.5		4616.7
4703				783.8			
4704				1652.7			
4705							545.2
4801	4656.5	5356.3	5215.6	9642.7	4324.9	5417.7	8165.9
4802	5843.9	15440.9	18369.3	11950.9	4136.0	9578.6	18997.4
4803	2552.6	1627.4	1539.5	2688.1	2509.8	6534.1	8596.9
4901				1043.6	489.1	821.6	
4902				980.1		1681.3	
5001							
5002	1986.7	2567.3	1525.2	1274.9		1157.2	
5003							4881.3
5101							33313.1
5102	1724.0	1264.9		1153.2	1704.3	1312.9	
5103				1394.8	1794.1	2014.7	820.0
5104							1762.8
5105							
5201	3506.0	1786.0		509.0	1358.8	2327.2	1388.0
5202	2683.3	2831.0	1264.1	1616.6	2974.0	2152.9	1254.4
5203				3751.1			1126.7
5204	2123.2	3233.3			3388.8	4029.5	
5205							1066.4
5301	1074.5	827.3		691.6	1012.1	722.1	743.2
5302	8714.7	6528.2	6907.7	3670.6	3667.7	3942.7	2002.4
5401	1259.3	881.1		1227.9	1724.3	1836.3	813.8
5501	4142.5	3929.7	4286.8		3466.9	3621.9	1218.1
5502	1047.7	764.7	1024.1		930.0	517.2	525.0
5503	2104.9	2277.5		6734.6	5797.0	2896.8	5559.4
5504	129.3	201.3	104.2	155.4	317.5		
5506	5665.8	2998.8	5737.6	4414.2	5317.7	4327.6	972.1
5601	1604.1			3179.8			
5602		1583.1		706.3		1052.8	3154.6
5701	1789.7	3854.5	1352.8		3946.3	3582.2	2185.7
5702	1890.5	3008.5	2294.7	2435.1	3642.9	3681.5	754.8
5703				628.2	466.9		

5705	1315.5	767.8	1234.7				
5801			780.5	4142.9	1236.3	2783.6	
5802						1070.6	
5803		514.0		1162.8	1639.7	601.4	638.7
5804	2462.0	2131.5	2393.0	3979.4	4306.1	3980.0	647.8
5805				352.4		787.2	
5806	713.7		1582.9	1600.9	2084.8	1366.0	
5807	2516.8	5253.4			1904.6	1620.5	17091.3
5901		836.3		1747.7	1564.6	2572.2	
5902		1760.4		1238.2	2135.8	1477.9	
5903		654.1		531.4		573.0	
5904							
6001							3062.1
6101	950.3						2145.6
6102	15582.6	19803.2	17326.4	9939.8	9860.9	10905.5	11833.1
6103							3578.8
6104							
6201	1256.1	1692.7	1639.3	1146.2	1377.0	1237.8	768.2
6202		2294.7		1055.9			1060.9
6203		814.3	2074.9	741.0	860.0	825.1	
6204				530.6	608.6	825.3	2599.5
6205				2429.2		1526.3	1730.5
6301	5079.4	6931.3	2768.5	768.8	593.6	664.6	
6302							
6303	2299.8	3552.9	2817.9	2788.9	3352.6	3291.6	2772.2
6304		627.4		356.8	498.6	520.9	
6305	1762.0	687.0					1099.0
6401	1792.8	6176.6	3130.0	2495.9	3511.7	5009.2	2869.8
6402	4717.2	5407.4	5218.3	4514.2	4501.7	5440.4	1951.9
6403	1889.3	1438.6	962.8	870.6	1005.8	890.0	
6404				1275.8			
6501	827.7						480.5
6502	460.9		4798.6	844.5		606.1	
6601	566.8	729.0					
6602				552.3			
6701	594.8	384.9	799.9		1334.8	1019.9	
6702	3513.5	3360.9	4566.8	4148.8	3910.7	4066.2	1662.2
6703	185.1	435.2	443.4	1337.9	1449.9	757.1	747.3
6704	5155.5	5473.5	5225.0	4807.6	5988.0	6042.9	2431.7
6705	2754.3	3500.3	3152.6	3513.9	2956.4	2130.6	1745.3
6706							
6801	4416.7	2791.3	2930.6	2363.7	3943.8	3683.9	1497.5
6802							
6803							1538.1
6804							714.8
6805							464.0
6806	410.4	348.6	614.5				2663.2

6807	335.9		682.2				2741.6
6901		237.7					
6902	338.3	261.7	521.1	389.6	412.9	387.1	2578.1
6903							
7001	1122.2	976.2			698.5	769.0	
7002	1617.3	1036.5	900.0	1203.1	1334.6	1623.5	1087.0
7003	7798.9	5470.7	6984.8	5286.0	5728.8	4879.4	1955.5
7004	1734.1			3239.7	3240.8	2635.9	2551.6
7005							
7006	1142.2	1101.8					
7101	2584.1	1887.9	929.0	1785.4	2084.6	1231.2	1503.1
7201				369.1			
7301							
7302	2226.8			890.1	617.7		3091.9
7401		805.9					
7402	466.0	266.7	349.8	327.1	323.6		
7403							
7404							
7502	1460.3	1608.1	1372.5	3372.3	3183.3	2730.3	1719.1
7503	2979.2	1491.1	2320.4	3672.5	5342.0	2881.1	1024.1
7504	2561.4	4073.2					
7505	759.6					951.5	
7601	1483.6			844.2	1530.0	1744.7	
7602	1616.9	1027.1	956.8	1825.5	1451.8	1531.3	733.6
7603				1261.7	1539.1	1665.8	
7604	1397.7				2183.0	1174.5	772.7
7605	2156.6	1214.0	1271.2	2895.3	2788.8	2487.6	1212.5
7701	2505.8	2280.8	2759.0	1588.1	3332.6	2792.2	683.8
7702		286.2		1297.3	969.0	599.6	
7703	1458.7	1378.7	1358.8	734.1	664.0	704.3	
7704				880.3		609.9	
7705	850.9			587.1	1273.4	2308.3	
7706		668.1	722.7				
7707					877.0		
7708					472.9	821.2	
7709			139.4		836.8		
7801	404.8	421.5	670.1	689.0	728.3	1314.4	
7802	2173.3	1753.9	1967.9	1220.7	1663.4	1322.0	
7803							1485.5
7901					376.9		
8001	8530.5	3618.8	4675.8	3908.8	1554.1	1946.5	4124.2
8002	10442.5	8933.4	12846.8	5233.8	7047.0	6702.8	3366.0
8003	2535.0	2123.4	1708.1	1038.2	1122.2	1069.3	875.3
8004	2281.4		1107.2		536.7	786.8	
8005				816.4	1382.3	1183.6	
8006				1599.7		2970.0	
8007							394.4

8101	3381.4	2232.9	3202.3	1202.5	1334.9	1365.3	1582.5
8102	1770.5	1310.2	1314.5		2472.7	2275.9	
8103	1255.9	1684.0	1062.2	1070.2	986.4	1166.9	923.1
8201							
8202					613.4		
8203	2124.8	2518.3	1035.4	3809.1	2317.3	2050.1	895.8
8204				1284.5			570.3
8205	911.9						
8301	971.4	1006.1	959.3	686.1	1162.1	1310.7	544.7
8302	1816.6	1842.5	2255.3		3756.1	3545.1	
8303		1467.7		2865.8			
8401	1624.1	1027.5		2177.8	2201.0	3021.8	
8402	1194.4				1245.0		
8403	7695.4	2273.4	2075.2	9766.4	8129.8	19753.7	1068.8
8501	3173.5	1969.7	2188.2	1488.8	1694.2	3746.4	
8501	3173.5	1969.7	2188.2	1488.8	1694.2	3746.4	
8502	1248.0			2082.7	1942.5	2565.2	698.5
8601	712.9	811.4	769.1	611.9	1117.6	2768.9	
8602				643.0	1989.0	3895.6	
8603					1484.5		
8604				8022.4	2942.9	1974.3	
8701	1864.3	2572.1	1538.2	2473.9	2311.8	2631.3	1533.4
8702					1285.4	1685.5	
8703	715.7			6068.2	1993.5	4911.9	
8704				9980.3	2282.6	4793.3	
8705		578.7					
8706				553.5	813.2	890.9	
8707							
8801					481.1	619.3	
8802							
9001	9613.6	1048.0		7497.4	2132.3		5097.9
9002	1399.6	1538.0	1363.9	1753.2			
9003	4655.7	1248.3		2020.0	2325.0		
9005				1586.5	1177.6		
9006					1066.5		2013.8
9007							
9101							
9102							
9201	7273.5	2582.0	2560.3	8503.0	2412.4	12389.6	2192.8
9202				2173.0	856.8		
9203	5139.8	1093.8		2505.9	2920.4	4064.5	727.4
9204	3655.6			3856.3	2777.2	3043.1	4312.8
9205					515.3		
9301	4133.2	1174.0	1347.7	5843.3	2379.8	4273.8	1175.7
9302	4110.1				2874.7	4959.4	5515.9
9303					6475.3		
9304							

9401	7210.8	3164.7	2411.2	6932.4	8479.1	10255.5	1269.4
9402							4570.5
9501	1455.5			8124.6			1948.1
9502	3405.1	799.6		3746.9	4540.7	3616.3	
9503	3240.1	2478.0	4821.8		2139.0		
9601	15041.2	4030.7	3176.4	17929.7	20003.4	32059.1	12643.7
9602	30212.3	27302.6	42945.1		19962.8		
9603							
9604			14535.6	4758.0		12792.0	
9701	4297.5	1842.3	1766.4	5311.9	3951.2	4553.3	735.7
9702	8966.6	8670.0	12374.4		2943.9		
9801	3407.3	786.6		5808.9	3710.2	5226.0	1097.6
9802					3345.0		

d5r2	d5r3	d7r1	d7r2	d7r3
26947.9	13465.4	19266.7	27975.9	23030.8
3531.8	535.4	2791.7	2874.1	3050.9
6533.7	1516.4	3918.8	6586.4	5121.3
1226.2		1664.6	1158.5	1376.3
27363.2	11318.7	16486.9	22311.3	18914.1
709.2		2257.5	1095.5	1634.6
1537.5	775.7		735.5	717.1
		2227.6		2171.9
4488.8	2006.1			
	1163.0			
	6353.2	3431.0		3345.3
22194.7	9047.0	16005.5	15434.7	15327.1
4221.4	1405.7	2790.0	1430.1	2057.4
	6591.0	693.1	1079.8	864.4
			1118.4	1090.5
5902.2			582.9	568.4
14222.8	92084.7	6688.1	4585.9	5496.1
2228.7	845.4	2124.1	1702.9	1865.7
			1092.2	1064.9
807.4	334.1	226.5	396.6	303.8
6064.8	2106.0	5345.8	10070.1	7515.3
14154.8			15198.0	14818.1
1167.6		1327.3	3191.9	2203.1
17111.4	4027.2	45673.0	42530.1	42999.1
26042.4		13166.5		12837.4
		2317.8		2259.9
		1587.6		1547.9
		1840.1		1794.1
		830.2		809.5
		914.7		891.9
		806.4		786.3
1955.9		955.8	902.1	929.0
9135.9		4120.0	15747.1	9685.3
1240.5			2774.7	2774.7
		4556.2		4442.3
805.7			1562.3	1523.3
12625.1		4109.0	4353.9	4125.7
32054.2			7851.6	7655.3
	563.1	4477.7	8633.1	6555.4
8742.6	22144.8	54071.8	40370.4	47221.1
2649.8			2711.7	2643.9

685.2			1078.1	1051.2
1822.0			2052.6	2001.3
1608.7	1545.0	763.2	1363.8	1063.5
23870.8	18236.1	17124.6	30350.4	23537.5
	5485.0			
12337.5	14036.7		11166.7	10887.6
		2792.1	2579.6	2902.9
82122.1	37019.0	126844.5	180254.4	149710.8
	32665.5			
5519.0				
		21606.6		21066.5
56537.2		16109.1		15706.4
2664.0	391.2		1546.8	1508.2
10250.0	330.3			
4197.6		997.1		972.2
1162.9	283.2		1592.3	1552.5
1379.4			2172.2	2117.9
2337.2	570.0	6615.3	6746.1	6680.7
		2502.5	984.5	1699.9
		1578.6		1539.2
	436.4	1216.2	1172.6	1164.6
		1732.3	1235.3	1483.8
	1014.0	5033.3	3490.8	4155.6
5899.5	8039.9	7681.2	12082.3	9634.8
13514.6	12089.0	17686.7	24706.4	20666.7
3540.8			1455.9	1419.5
2183.3		11594.4	10921.2	11342.8
7131.4	4153.1	10379.9	17575.5	13628.3
		2608.4		2543.2
1494.3	377.8	1759.8	1760.2	1760.0
6618.8	2891.8	3469.7	6643.6	4930.3
4995.9	4212.1	4786.6	6361.2	3573.9
7069.7	2901.2	7182.1	7791.5	7486.8
		1556.2		1517.3
4140.6	45284.7	1447.8	1753.2	1560.5
524.6			489.9	477.7
6090.3	10657.4			
12791.5	5659.1	1002.7	9590.9	5296.8
5218.0	2936.1	2198.4	4284.7	3241.6
11181.3	4276.6	6508.9	9575.8	8142.4
1862.4	557.8		526.9	513.8
		693.8	1432.9	1036.8
1662.1	1039.0			

741.8	837.3	991.8	2054.3	1485.0
	625.6		1016.5	991.1
2684.0	350.6		6452.4	6452.4
1752.4	9458.3		2047.3	1996.1
3413.0	1222.1		5692.4	5692.4
999.8	658.9	7168.7	2477.9	4702.7
	5698.4			
1128.0	2449.4	4984.5	3647.0	3425.8
969.5			2366.4	2307.3
670.2	520.0	1024.0	1472.2	1248.1
913.2			1058.6	1032.2
		344.2		335.6
1497.4	376.0	4204.3	5056.0	4514.5
2100.3	823.3	3666.5	3269.9	3381.5
		4734.1	4337.3	4127.7
438.8		1944.8	1662.3	1758.5
1303.9		1394.9	1334.8	1330.8
435.7			611.3	596.0
			182.7	182.7
3647.2		2743.0	2894.3	2893.7
		1626.3	978.3	1202.3
303.4			1039.0	1013.1
692.0	693.8		4215.0	4109.7
975.6		2249.9	2279.2	2264.6
2860.0	2583.3		868.7	868.7
		3526.4		3438.3
		3128.4		3050.2
	1997.7	582.8		568.3
4901.5	6995.6	14637.5	21317.6	17977.6
1770.8	2788.8		2042.5	2042.5
3583.9		8505.8	6415.3	7440.6
	1661.7	1750.8	1232.2	1491.5
8130.3	1725.5	11932.0	11311.7	11093.9
1131.9		1470.5		1570.5
718.8		711.7	595.6	637.4
2491.8	24835.3	582.4	1194.4	866.2
		1183.3	1190.3	1157.2
5823.4	2070.4	3239.3	6311.9	4656.2
		799.6		779.6
		3258.5	405.7	1786.3
938.9			1868.6	1821.9
		2004.1		1954.0
		763.4		744.3
1586.5	681.9		1397.6	1377.6
		2974.4	1036.1	1955.2

1424.6	221.8	526.3	1390.4	958.4
5216.0	106999.1	566.5	3797.7	2127.6
6230.3	1859.9	4738.2	4566.3	4536.0
2745.5		1104.6	3194.9	2096.1
8614.4		2142.8	4090.5	3038.8
2470.2	9932.5	2715.2		2647.3
3853.0	17199.1	3255.2	4201.5	3728.4
2451.8			3157.5	3078.6
			363.2	354.1
		4132.7		4029.4
1444.2		13598.4	1417.9	7320.5
2637.3				
		18259.5		17803.0
		7807.1		7611.9
671.7	654.6	457.5	863.4	644.0
7698.6	9355.2	7597.6	7048.9	7028.9
20670.4	27507.1	16494.1	7132.0	11517.8
5316.7	99932.6	2383.9	5629.5	4006.7
		1161.9	1091.0	1126.5
	2262.5			
4307.3	34363.9		1184.6	1155.0
1126.5	3797.1	800.2	1136.0	943.9
	2523.9			
749.6		581.1		566.6
3050.8		2727.4	1537.8	2079.3
2548.4	270.2	2194.3	1537.7	1819.4
			1701.5	1659.0
3970.8	497.0	2077.6	2439.4	2202.1
	610.9			
1483.1	493.2	1454.5	1545.0	1462.3
2929.6	960.8	1963.8	1789.7	1876.8
1717.4		1541.7	945.2	1212.4
2683.4	820.9	1871.6	2588.9	2230.3
416.1	647.0		594.6	594.6
2164.7	9692.8		2434.4	2434.4
224.1		2065.9	2256.9	2159.9
3520.0	1387.8	2119.7	7689.1	4904.4
1156.2			485.9	473.8
1143.2	3698.3		1318.1	1285.2
2724.9	3170.4	1735.5	4006.6	2799.3
2416.1	2570.2	1188.5	1143.1	1165.8

1118.4	1080.4	465.7	499.5	470.6
1095.0	2024.6		865.5	865.5
	391.2		640.4	624.4
1372.8	394.1	508.5	1047.6	728.1
1514.5	740.5	868.4	1053.6	961.0
			321.8	313.8
5135.9	19507.4		493.8	481.5
5260.4		2612.2		2546.9
			507.1	494.4
	1683.8			
1166.9		767.4	1025.1	873.9
18716.0	5168.7	12428.1	15833.4	14130.8
	6443.5			
		1275.2		1243.3
1833.3	314.5	1229.0	967.6	1070.9
1797.7	635.7	715.8	801.2	739.6
624.9	2788.8	828.3		807.6
2738.5			1873.9	1827.1
927.3		546.8	602.3	560.3
960.6			453.6	442.3
4822.4	1345.5	3728.9	3531.6	3539.6
832.5	194.2	629.2	489.4	545.3
2747.5			1338.1	1304.7
6772.5	1047.2	4511.2	1088.9	2730.1
5351.3	1242.0	3051.8	5645.7	4348.8
		1107.0		1107.0
834.7	345.9			
			490.8	478.6
778.8		604.9	656.5	615.0
712.9		611.3		596.0
559.9	244.3			
			558.4	558.4
2772.4	744.2	2601.1	2761.3	2651.2
513.3	192.8		965.0	965.0
5426.3	1760.1	3060.5	2960.8	3060.7
2263.2	1309.5	1548.3	1322.5	1322.5
		804.4		784.3
575.6		1280.8	2250.8	1765.8
			769.8	750.6
233.9	3017.3			
	783.5			
	714.9			
555.1	3968.9			

	5315.5		102.2	99.7
605.7				
605.4	4845.6	440.6		429.6
			260.4	253.9
		770.5	763.6	747.9
1235.4	713.9		1372.6	1338.3
3224.0	1189.0	5781.2	3709.6	4545.4
3034.7	870.6	1035.8	3975.4	2505.6
661.4			785.9	766.3
		1059.9		1033.4
2847.7	698.5	2201.2	2575.7	2328.8
		415.7		405.3
			1162.4	1133.4
3066.1	1628.2	1190.0	2361.4	1731.3
3230.8			653.1	636.8
659.0			435.2	424.3
	265.8		422.2	411.7
			416.1	405.7
4316.6	1012.2	1632.6	2583.5	2055.4
2583.0	815.1	1720.1	2583.8	2152.0
		773.9		754.6
	400.2		549.0	535.3
1340.8	622.2	606.7	773.8	690.3
2180.3	390.0		546.4	536.4
635.6	518.1	723.2	736.5	729.9
1154.3	851.0	1126.8	1425.3	1276.1
1654.3	667.7	1390.7	1750.5	1570.6
1034.3	204.1		744.9	744.9
538.4	144.7	911.4	775.4	843.4
581.1				
	405.2			
			520.9	507.9
			351.7	342.9
			320.9	312.9
			294.7	287.4
	214.6		550.3	550.3
588.1	569.3	713.0	1172.1	919.1
	1954.2			
3206.3	695.9	5181.7	3758.9	4420.3
5969.7	1271.5	9519.5	6438.9	7779.7
1462.1		3044.8	2433.1	2739.0
		667.8		651.1
370.6				
		782.5		763.0

1841.6	342.1	2487.8	2530.0	2508.9
865.5	407.7	1174.4	1192.8	1183.6
425.2	420.4	1312.4	593.6	1125.0
		413.4	704.6	559.0
			507.2	494.5
945.8		1524.2	957.0	1547.5
749.4				
627.0		822.7		802.2
1047.1	297.5	839.1	1404.1	1093.6
1817.3		1975.7	1114.3	1506.4
			1132.9	1104.6
796.0		1025.1	1743.8	1349.9
			630.6	614.9
5363.9	1936.0	5280.7	5325.5	5303.1
1129.3	608.2	780.2	830.6	805.4
1129.3	608.2	780.2	830.6	785.3
879.7			1182.3	1152.8
786.1	1521.3	687.0	595.0	631.0
		510.7	1018.5	745.5
	566.9		916.2	893.3
1899.8	1484.9	3394.8	3639.0	3516.9
			513.0	500.2
448.9			861.6	861.6
			680.0	663.0
				0.0
			353.3	344.5
		258.2		251.8
3069.4	1337.6	3068.3	4023.2	3457.2
		1396.2		1361.3
	495.3	1906.8		1859.2
		1112.8		1085.0
		1657.9		1616.5
		1119.2		1091.2
2712.6	1273.7	2197.9	1948.4	2073.2
695.8		1198.8	591.9	873.0
2449.6	1528.7	2086.0	2882.3	2422.1
	1031.1	3084.3	2079.2	2517.3
1270.3		1990.1		1940.4
2721.8	1075.5	3051.9	2990.2	3021.1
4567.2	2308.6	1557.6	4776.0	3087.7
	2820.3	3216.9		3136.5
		2950.0		2876.3

8086.0	4556.9	4055.0	2424.4	3249.7
			5077.4	4950.5
1983.7	947.2	1311.3	909.9	1082.9
		980.5	1507.6	1213.0
7011.4		5490.6		5353.4
11596.9	14722.3	5217.0	12605.8	8688.6
34154.7		21706.7	11204.5	16044.2
			1278.8	1246.9
		5554.4		5415.6
2111.9	863.1	1678.8	2063.4	1824.3
9307.5		5812.2	4873.4	5209.3
1227.5	1040.2	1001.9	2111.4	1517.8
1533.1			2403.9	2343.8